

بِسْمِ اللَّهِ الرَّحْمَنِ الرَّحِيمِ

Statistical Analysis of Burr Formation in Low Speed Micro-Milling of Titanium Alloy (Ti-6Al-4V)



Author

GULFAM UL REHMAN

MS (Design and Manufacturing Engineering)

NUST201362018MSMME62013F

Supervisor

Dr. Syed Husain Imran Jaffery

Co-supervisor

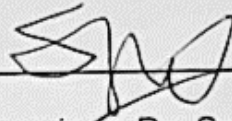
Dr. Mushtaq Khan

Department of Design and Manufacturing Engineering
School of Mechanical and Manufacturing Engineering (SMME)
National University of Sciences & Technology (NUST)
Islamabad, Pakistan
(December, 2016)

THESIS ACCEPTANCE CERTIFICATE

Certified that final copy of MS/MPhil Thesis written by Mr. GULFAM UL REHMAN, (Registration No. NUST201362018MSMME62013F), of School of Mechanical and Manufacturing Engineering (School/College/ Institute) has been vetted by undersigned, found complete in all respects as per NUST Statutes /Regulations, is free of plagiarism, errors, and mistakes and is accepted as partial fulfillment for award of MS/MPhil Degree. It is further certified that necessary amendments as pointed out by GEC members of the scholar have also been incorporated in the said thesis.

Signature: _____



Name of Supervisor: Dr. Syed Husain Imran

Date: 30-12-16

Signature (HOD): _____



Date: 30-Dec-16

Signature (Principal): _____

Date: _____

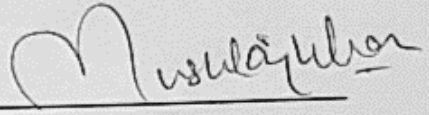
National University of Sciences & Technology

MASTER THESIS WORK

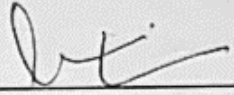
We hereby recommend that the dissertation prepared under our supervision by **GULFAM UL REHMAN** (NUST201362018MSMME62013F) titled: **Statistical analysis of burr formation in low speed micro-milling of titanium alloy (Ti-6Al-4V)** be accepted in partial fulfillment of the requirements for the award of MS Design and Manufacturing Engineering degree with (A) grade.

Examination Committee Members

1. Name: Dr. Mushtaq Khan

Signature: 

2. Name: Dr. Liaqat Ali

Signature: 

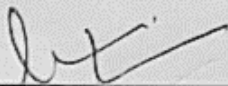
3. Name: Dr. Shahid Ikramullah

Signature: 

Supervisor's name: Dr. Syed Husain Imran

Signature: 

Date: 30-12-16



Head of Department

30-Dec-16

Date


COUNTERSIGNED

Date: _____

Dean/Principal

DECLARATION

I certify that this research work titled "*Statistical Analysis of Burr Formation in low speed micro-milling of Titanium Alloy (Ti-6Al-4V)*" is my own work. The work has not been presented elsewhere for assessment. The material that has been used from other sources it has been properly acknowledged/referred.



GULFAM UL REHMAN
(NUST201362018MSMME62013F)

COPYRIGHT STATEMENT

Copyright in text of this thesis rests with the student author. Copies (by any process) either in full, or of extracts, may be made only in accordance with instructions given by the author and lodged in the Library of SMME, NUST. Details may be obtained by the Librarian. This page must form part of any such copies made. Further copies (by any process) may not be made without the permission (in writing) of the author.

The ownership of any intellectual property rights which may be described in this thesis is vested in SMME, NUST, subject to any prior agreement to the contrary, and may not be made available for use by third parties without the written permission of SMME, NUST, which will prescribe the terms and conditions of any such agreement.

Further information on the conditions under which disclosures and exploitation may take place is available from the Library of SMME, NUST Islamabad.

ACKNOWLEDGEMENT

This Thesis work has been done at School of Mechanical and Manufacturing Engineering (SMME) at NUST, Islamabad under the project “*Statistical Analysis of Burr Formation in Low Speed Micro-Milling of Titanium Alloy (Ti-6Al-4V)*” and is submitted in partial fulfillment of the requirements for the degree of Master of Science program in Design and Manufacturing (DME) at SMME, NUST University.

Firstly, I would like to thank **Allah Almighty** and express my sincere gratitude to my advisor **Dr. Syed Husain Imran** for continuous support of my MS study and related research, for his patience, motivation and immense knowledge. His guidance helped me in all the time of research and writing of this thesis. I could not have imagined having a better advisor and mentor for my MS study.

Besides my advisor, I would like to thank the rest of my thesis committee: **Dr. Mushtaq Khan, Dr. Liaqat Ali, Dr. Shahid Ikramullah, Dr. Samiur Rahman** and **Dr. Muhammad Safdar** for their insightful comments and encouragement, but also for the hard question which incited me to widen my research from various perspectives.

I also acknowledge the help of **Dr. Masood Shah, Engr. Faisal Qayyum, Engr. Muhammad Imran** and **Engr. Zaheer Ahmed** from UET Taxila to let me utilize Scanning Electron Microscope. I also would like to thank **Dr. Amir Jaleel** for guiding me along the right path throughout my research and CNC machine operators **Mr. Waseem, Mr. Akseer** along with MRC shop officials and operators for making the working in the laboratory a joy.

I thank my fellow research mates SMME, NUST for the stimulating discussions. In particular, I am grateful to **Engr. Sohail Akram, Asst Prof. Salman Sagheer Warsi, Engr. Usman Abdullah, Engr. Muhammad Farooq** and **Engr. Nauman Khan** for their support and time during the experiments and thesis writing.

Last but not the least, I would like to thank my family for their never ending support and encouragement through very difficult times to complete research work. Especially my **mother and father** who pray for me every second.

DEDICATION

To my Beloved Parents,

*Without whom none of my success
would have been possible*

&

To my Respected Teachers,

*Who acted like compass
that activated the magnets of
curiosity, knowledge and wisdom in me*

ABSTRACT

Increasing demand of micro scale components in the industry of electronics, aerospace, automotive and biomedical has opened up a door where there is strong research potential in the field of micro machining. Titanium based alloys are the most suitable to be used as workpiece material for different applications in these industries. Out of actual titanium usage, Ti-6Al-4V accounts for more than 45%. On one side, it exhibits strong properties like biocompatibility and excessive strength to light weight ratio while on the other side, it is very hard to machine due to low thermal conductivity and high chemical reactivity.

In this research, feed per tooth, conventional cutting speed and depth of cut are considered as machining parameters and their effect on burr formation is analyzed through statistical technique of analysis of variance to determine key process variables. Results showed that feed per tooth is the most dominant factor causing burr formation (81% contribution ratio), cutting speed is second dominating factor (6% contribution ratio) and impact of depth of cut is negligible (1% contribution ratio). Results also show that micro-milling machining process is sensitive to residual effect (12% contribution ratio). Machining at optimum process parameters showed minimum burr formation. Although conventional speed micro-milling of titanium alloy would take more time than high speed micro-milling but it would give better results in terms of minimization of burr.

Keywords: Micro-machining, low speed, Titanium Alloy, Ti-6Al-4V, statistical analysis, burr formation, top burr, micro-milling, ANOVA

TABLE OF CONTENTS

LIST OF FIGURES	I
LIST OF TABLES	III
NOMENCLATURE	IV
CHAPTER 1	1
INTRODUCTION	1
1.1 <i>Research Motivation</i>	2
1.2 <i>Research Objectives</i>	2
1.3 <i>Research Scope</i>	3
CHAPTER 2	4
LITERATURE REVIEW	4
2.1 <i>Micro-machining advantages</i>	4
2.2 <i>Micro-Milling</i>	5
2.3 <i>Titanium Alloy</i>	6
2.4 <i>Machining of Titanium alloys</i>	7
2.5 <i>Micro-milling vs Macro-milling</i>	11
2.6 <i>Micro-milling Applications</i>	14
CHAPTER 3	20
METHODOLOGY	20
3.1 <i>Experimental Design</i>	20
3.2 <i>Selection of Parameters</i>	21
3.3 <i>Experimentation</i>	23
CHAPTER 4	24
RESULTS AND DISCUSSION	24
4.1 <i>SEM Images</i>	25
4.2 <i>ANOVA (Analysis of Variance)</i>	29
4.3 <i>ANOVA Calculations</i>	30
4.3 <i>Burr Formation Analysis</i>	34
4.4 <i>Confirmation test</i>	36

CHAPTER 5	39
CONCLUSIONS	39
<i>5.1 Recommendations</i>	39
REFERENCES	41

LIST OF FIGURES

Figure 1 Accuracy vs scale for the micro mechanical machining [1] -----	1
Figure 2 Development of achievable machining accuracy [11] -----	6
Figure 3 Distribution of thermal load when machining titanium and steel [14]-----	8
Figure 4 Normal and tangential stresses in machining [14]-----	9
Figure 5 Schematic of macro and micro milling process [3] -----	12
Figure 6 Micro-milling tool workpiece interaction [6]-----	13
Figure 7 Types of milling Burrs [24] -----	14
Figure 8 (a) Lab-on-a-chip; (b) Microplate with 96 capillarity electrophoresis system (vacuum hot-embossing plate from micro-milled mould) and filling of one structure; (c) Medicine micro-dosage system; (d) Sweat-stick for collecting human sweat [3] -----	16
Figure 9 (a) Integrated polymer microfluidic stacks (chemiluminiscence experiment); (b) Dental brackets; (c) Tissue removal tools for endoscopy; (d) Cataract lenses; (e) Fabrication of Ti retinal microtack [3]-----	17
Figure 10 (a) Engraving watch base plate; (b) Watch parts; (c) Pendant mould [3]-	17
Figure 11 (a) Injection nozzles for diesel engines; (b) Electrodes for cutting inserts [3] -----	18
Figure 12 (a) Multi-fibre connector (micro-milled mould for X-ray mask fabrication and microinjected connector); (b) Joining element for optical fibre connector; (c) Test membrane for computer chip manufacturing [3] -----	18
Figure 13 (a) Mixing disc of a rocket motor; (b) Turbine wheels for microfluidic pumps; (c) Micro-mould of a planetary gear wheel; (d) Assembled micro impeller and base block [3] -----	19
Figure 14 Experimental Setup (1) Spindle; (2) Micro-end mill; (3) Workpiece; (4) Machining vise; (5) Magnified view of tool and workpiece -----	21
Figure 15 Workpiece after micro-milling -----	23
Figure 16 Top burr width measurement -----	24
Figure 17 Burr formation at down milling and up milling side -----	25
Figure 18 Scanning Electron Microscope (SEM) -----	25
Figure 19 SEM images at $f_z = 8 \mu\text{m/tooth}$, $V_c = 5 \text{ m/min}$, $a_p = 50 \mu\text{m}$ -----	26
Figure 20 SEM images at $f_z = 8 \mu\text{m/tooth}$, $V_c = 7.5 \text{ m/min}$, $a_p = 75 \mu\text{m}$ -----	26

Figure 21 SEM images at $f_z = 8 \mu\text{m/tooth}$, $V_c = 10 \text{ m/min}$, $a_p = 100 \mu\text{m}$ -----	26
Figure 22 SEM images at $f_z = 10 \mu\text{m/tooth}$, $V_c = 5 \text{ m/min}$, $a_p = 75 \mu\text{m}$ -----	27
Figure 23 SEM images at $f_z = 10 \mu\text{m/tooth}$, $V_c = 7.5 \text{ m/min}$, $a_p = 100 \mu\text{m}$ -----	27
Figure 24 SEM images at $f_z = 10 \mu\text{m/tooth}$, $V_c = 10 \text{ m/min}$, $a_p = 50 \mu\text{m}$ -----	27
Figure 25 SEM images at $f_z = 12 \mu\text{m/tooth}$, $V_c = 5 \text{ m/min}$, $a_p = 100 \mu\text{m}$ -----	28
Figure 26 SEM images at $f_z = 12 \mu\text{m/tooth}$, $V_c = 7.5 \text{ m/min}$, $a_p = 50 \mu\text{m}$ -----	28
Figure 27 SEM images at $f_z = 12 \mu\text{m/tooth}$, $V_c = 10 \text{ m/min}$, $a_p = 75 \mu\text{m}$ -----	28
Figure 28 Main effects plots for top burr width with respect to machining parameters -----	34
Figure 29 Main effect plot between top burr width and f_z/r_e -----	35
Figure 30 Main effect plot between top burr width and f_z/r_e [6]-----	36
Figure 31 Scanning Electron Microscope image at optimum conditions (Run 1) ----	37
Figure 32 Scanning Electron Microscope image at optimum conditions (Run 2) ----	37
Figure 33 Scanning Electron Microscope image at optimum conditions (Run 3) ----	38

LIST OF TABLES

Table 1 Chemical composition of Titanium 6Al-4V (wt %)	10
Table 2 Mechanical properties of Titanium 6Al-4V.....	10
Table 3 Physical properties of Titanium 6Al-4V	10
Table 4 Experimental conditions.....	20
Table 5 Process parameters.....	21
Table 6 L9 array (RPM and feed speed).....	23
Table 7 L9 array (cutting tests with measured outputs)	29
Table 8 ANOVA table for top burr width	34
Table 9 Experimental results at optimum conditions.....	38

NOMENCLATURE

Symbol	Abbreviation	Symbol	Abbreviation
r_e	Tool edge radius	KPVs	Key Process Variables
D	Tool diameter	BCP	Body centered cubic packing
r	Tool radius	HCP	Hexagonal Closed Packing
Z	Number of flutes	2D	Two Dimensional
V_c	Cutting Speed	3D	Three Dimensional
V_f	Table speed	df	Degree of freedom
a_p	Axial depth of cut	EDM	Electro Discharge Machining
a_r	Radial depth of cut	CR	Contribution ratio
f_z	Chip Load or feed per tooth	SEM	Scanning Electron Microscope
rpm/N	Revolutions per minute	SS	Sequential sum of squares
μm	micrometer	Al	Aluminium
g/cm^3	gram per centimeter cube	Cr	Chromium
HB	Brinell Hardness	Cu	Copper
m/min	meter per min	Fe	Iron
mm	millimeter	Mn	Manganese
$\alpha + \beta$	alpha-beta	Ti	Titanium
GPa	gigapascal	V	Vanadium
MPa	megapascal		

INTRODUCTION

As technology is moving forward and trying to reduce the size of components as much as possible, manufacturing operations and techniques are shifting their focus towards small scale components. With the increasing demand of small scale components, research needs to be done at micro and nano scale. Micromachining, which includes micro-scale milling, turning and drilling, are processes that remove material in the form of chips and within the dimensions of 0.1 μm to 100 μm . Highly precise instruments and equipment are required to maintain the increased accuracy of small scale components. Fig. 1 shows the position of micro machining, in terms of scale and accuracy, with respect to other machining processes which are used to remove material. For the last 2 decades, a lot of research has been done on macro machining tools, processes, techniques and materials and moving towards micro domain is not as simple as scaling down properties of macro domain. So, new research should be performed in order to understand the micro machining technicalities.

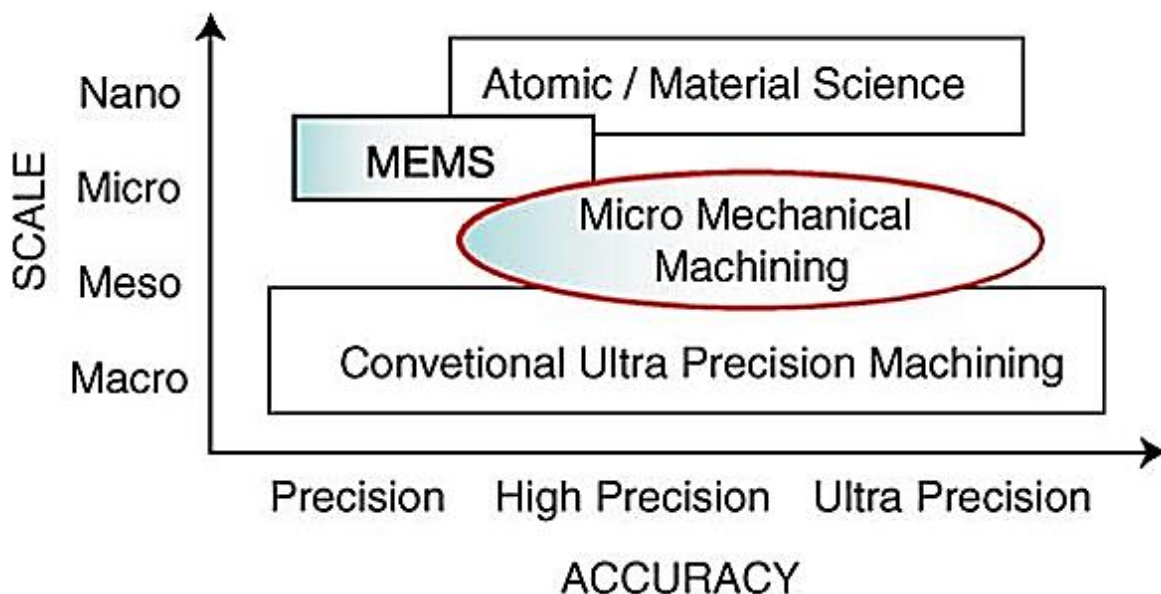


Figure 1 Accuracy vs scale for the micro mechanical machining [1]

As the demand of micro components is increasing, the need for accuracy and precision of micro features is also increasing. In increasing research, this is the major driving force.

1.1 Research Motivation

Mechanical machining is always accompanied by burr formation either it is macro-machining or micro-machining. Deburring in macro-machining is easy as compared to micro-machining. In micro components deburring, may destroy delicate micro features as well as it can damage the workpiece. Moreover cost of deburring process is very high as it requires complex assembly operation [1–3]. So, it is undesirable to use deburring process to minimize burr.

Bajpai et al. analyzed burr formation in micro-milling of Ti-6Al-4V by varying cutting speed between 16 m/min and 141 m/min and 16 m/min is the minimum cutting speed so far reported in the literature [4]. Jaffery et al. statistically analyzed the machining parameters in micro-milling of Ti-6Al-4V and it is evident from results that although high speed in micro-machining has many advantages but cutting speed has very less contribution as compared to feed rate on burr formation [5]. So, instead of using high speed machining setup, low speed machining setup could be used which is easily available and economical while high speed machining setup is expensive.

Therefore, using carbide tools for micro-milling of Ti-6Al-4V, this study aims to find out effect of critical machining parameters namely, feed rate, low cutting speed and depth of cut on burr formation and use statistical technique to find out best combination of key process variables (KPVs) to minimize burr formation.

1.2 Research Objectives

The main objectives of the research are:

- Analysis of burr formation at different cutting parameters
- Find out the influence of each parameter using statistical analysis tool ANOVA
- Select the optimum level of each parameter and validation of experiments

1.3 Research Scope

The scope of this research is limited to micro end milling of Titanium Alloy Ti-6Al-4V using tungsten carbide tools at machining speed less than 8000 rpm.

LITERATURE REVIEW

Micro machining is a process used for manufacturing miniaturized parts and features. Demand for highly precise and accurate micro components is rising day by day in the industries i.e. biomedical, aerospace, automotive and electronics [5]. “This miniaturization will provide micro-systems that promise to enhance health care, quality of life and economic growth in such applications as micro-channels for lab-on-chips, shape memory alloy ‘stents’, fluidic graphite channels for fuel cell applications, sub-miniature actuators and sensors, and medical devices” [6]. There are few unconventional machining processes which could be used to produce micro scale components such as micro electro-discharge machining (micro EDM), micro-laser machining, focused ion beam cutting and micro-forming, but these machining processes have limitations either because of producing two dimensional (2D) micro-structures or high costs [7, 8]. Other than these, micro-milling is another unconventional machining technique which is capable of fabricating miniaturized three dimensional (3D) complex shapes. Although micro-milling is considered better than other non-traditional machining operations in terms of high material removal rate, process flexibility, low set up cost and producing complex shapes but it is also accompanied with some problems such as burr formation, low surface quality, unpredictable tool breakage, chip load and rapid tool wear. So, it becomes difficult to obtain desired results in micro-milling than that of macro-milling [1, 9].

2.1 Micro-machining advantages

Micro-machining also poses general advantages in different aspects of manufacturing, such as environmental, economic, and technical

2.1.1 Environmentally

- Saving energy and material resources: require minimum lubrication and no masking materials.
- Reduced vibration and noise for workers.

- Easier control of waste and pollution: removed material is contained in machine.

2.1.2 Economically

- Reduced need for capital investment such as land space, buildings and power, and doesn't require clean room upkeep.
- Reduced running costs: low power consumption, no need for high energy laser or x-ray technology.
- Efficient space utilization: small apparatus.
- Portability and reconfigurability: size of machines improves mobility.

2.1.3 Technically

- Higher speeds and accelerations, reduce inertia due to tool size
- Precision: micro and nano-scale
- Productivity: high allocations of machinery due to space consumption of machines
- Piece by piece process advantage, likely hood of faults can be monitored and improved quickly without loss of batches since batches don't rely on single mold.

2.2 Micro-Milling

Micro-machining is a method for manufacturing components and devices with features that range between tens of microns to few millimeters [6]. Micro-milling as a material removal process is becoming popular in the manufacturing industry. Micro-end milling has many advantages over other material removal processes in the micro domain such as process flexibility, ease of use and low overall cost. This type of material removal is very desirable in fields for small functional components such as medical devices [10].

Micro milling is expressed in terms of four parameters: Cutting speed, chip load, radial depth and axial depth. The cutting speed (V_c) is the linear speed of the cutting tip at the circumference of the tool. The chip load (f_z) is the proposed thickness of the chips that will be formed from each pass of a single cutting edge. The radial depth (a_r)

is the depth of the endmill into the workpiece in the direction parallel to the radius (r) of the micro-tool. The axial depth of cut (a_p) is the depth of the endmill into the workpiece in the vertical direction.

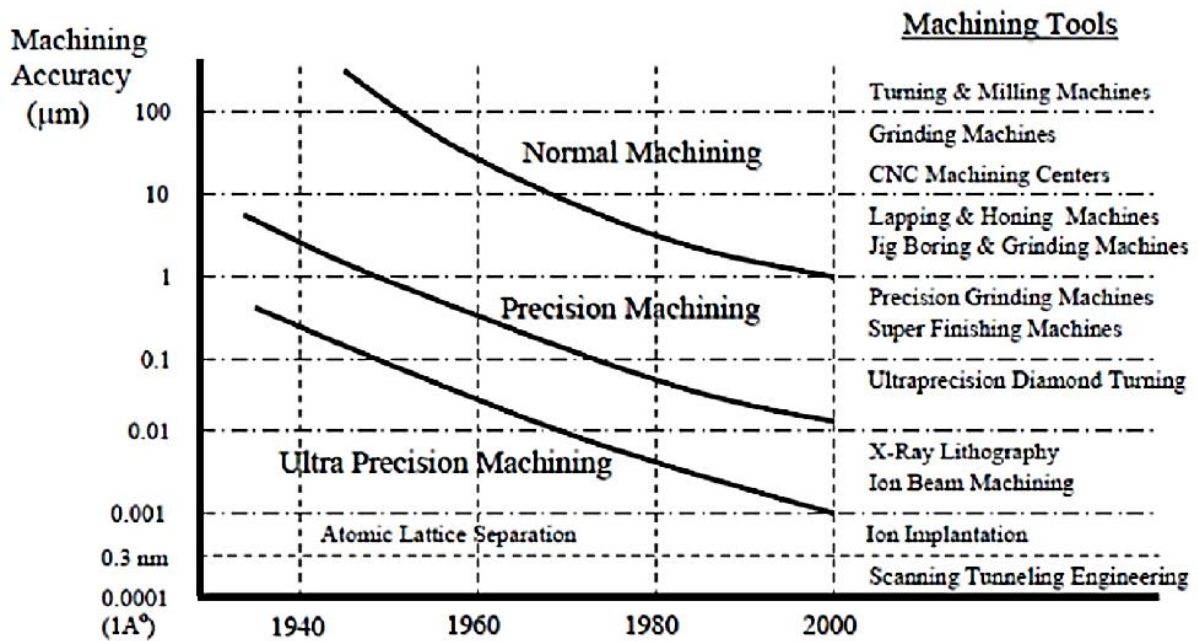


Figure 2 Development of achievable machining accuracy [11]

Fig. 2 shows that for normal machining, achievable machining accuracy is reaching the precision machining level. With more research, improved processes and techniques these curves would continue to move downward.

2.3 Titanium Alloy

Micro-milling becomes much more difficult when hard to cut materials are used for manufacturing such as Ti-6Al-4V titanium alloy [11]. Ti-6Al-4V is known by the name “workhorse” of the titanium industry as it accounts for more than 45% of actual titanium usage [5, 12]. It is widely used in biomedical (medical implants), aerospace (turbine blades, aerospace fasteners) and automotive (intake, engine and exhaust valves) and marine industry due to its excessive strength to light weight ratio, biocompatibility, corrosion resistance and property to withstand high temperature.

On the other side there are properties which makes it difficult to cut material such as low elastic modulus, high chemical reactivity and low thermal conductivity [3,

4, 10, 12–14]. Jaffery et al. observed that tool wear increases during the machining of Ti-6Al-4V due to its property of reacting chemically with cutting tool material (above 500°C) and high thermal resistance which leads to tool fracture as most of the heat generated goes into the cutting tool [15].

Ti-6Al-4V is an alpha-beta ($\alpha + \beta$) titanium alloy. This alloy contains both alpha and beta phases with alpha phase ranges between 60 to 90% and beta phase 10 to 40% at room temperature. Alpha phase consists of hexagonal closed packing (HCP) structure that remains stable from room temperature while beta phase is characterized by body centered cubic structure (BCP) which keeps it stable from room temperature to melting point. There are stabilizer elements adding which increase the stability of alpha and beta phase which lowers the transformation temperature of particular phase. For example adding aluminum, carbon, oxygen and nitrogen would increase the stability of alpha phase on the other side adding vanadium, molybdenum, manganese, chromium and iron would increase stability of beta phase [13].

2.4 Machining of Titanium alloys

Progress in the machining of titanium alloys has not kept pace with advances in the machining of other materials due to their high temperature strength, relatively low elastic modulus, high thermal resistance and high chemical reactivity. Therefore, success in the machining of titanium alloys depends largely on the overcoming of the principal problems associated with the inherent properties of these materials.

2.4.1 High cutting temperature

It is well known that high cutting temperatures are generated when machining titanium alloys and the fact that the high temperatures act close to the cutting edge of the tool are the principal reasons for the rapid tool wear commonly observed. As illustrated in Fig. 3, a large proportion (about 80%) of the heat generated when machining titanium alloy Ti-6Al-4V is conducted into the tool because it cannot be removed with the fast flowing chip or bed into the workpiece due to the low thermal conductivity of titanium alloys, which is about 1/6 that of steel. About 50% of the heat generated is absorbed into the tool when machining steel. Investigation of the

distribution of the cutting temperature has shown that the temperature gradients are much steeper and the heat-affected zone much smaller and much closer to the cutting edge when machining titanium alloys because of the thinner chips produced (hence short chip-tool contact length) and the presence of a very thin flow zone between the chip and the tool (approximately 8 μm compared with 50 μm when cutting iron under the same cutting conditions) which causes high tool-tip temperatures of up to about 1100°C [14].

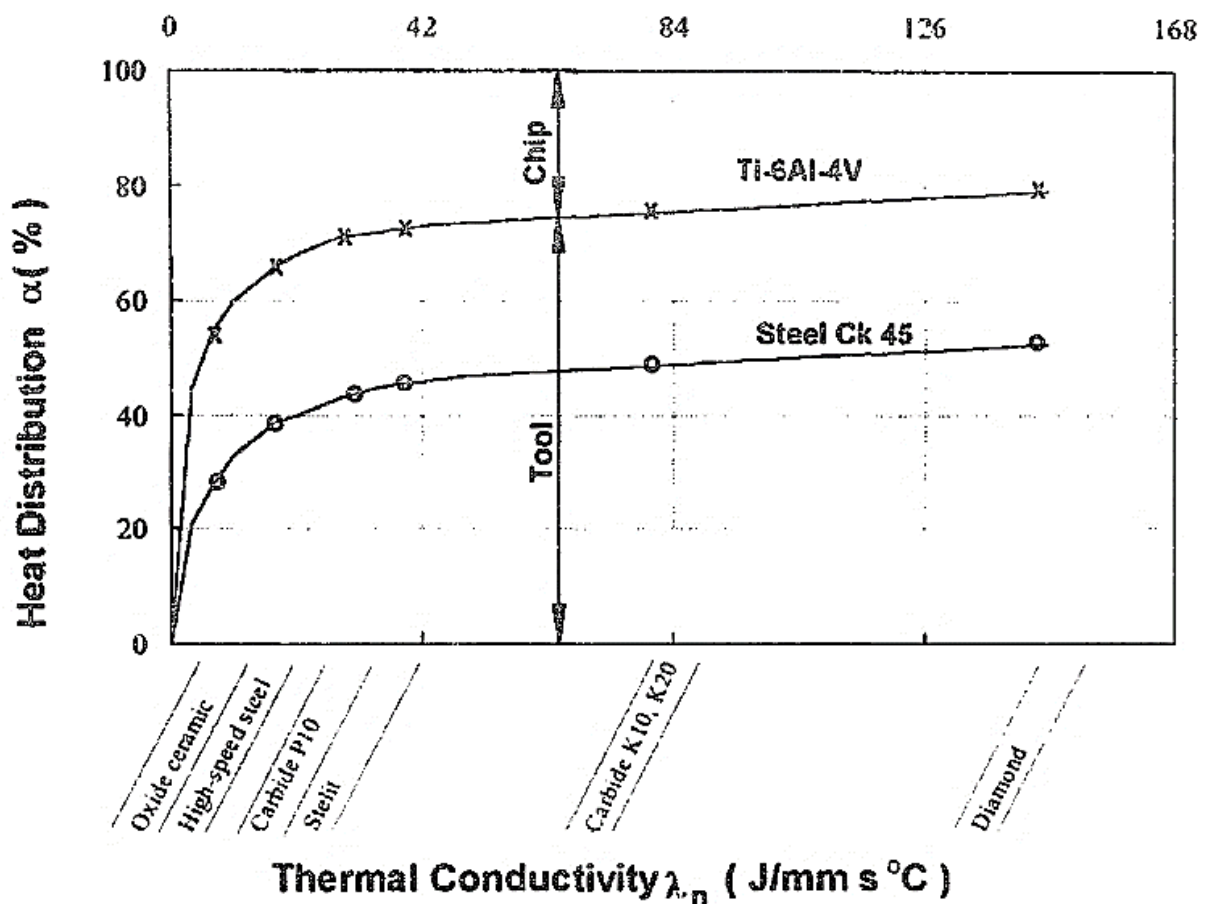


Figure 3 Distribution of thermal load when machining titanium and steel [14]

2.4.2 High cutting pressures

The cutting forces recorded when machining titanium alloys are reported to be similar to those obtained when machining steels, thus the power consumption during machining is approximately the same or lower. Much higher mechanical stresses do, however, occur in the immediate vicinity of the cutting edge when machining titanium alloy. Higher stresses on the tool have been reported when machining Ti-6Al-4V (titanium alloy) than when machining Nimonic 105 (nickel-based alloy) and three to

four times those observed when machining steel Ck 53N (Fig. 4). This may be attributed to the unusually small chip-tool contact area on the rake face, (which is about one-third that of the contact area for steel at the same feed rate and depth of cut) and partly to the high resistance of Ti-alloy to deformation at elevated temperatures, which only reduces considerably at temperatures in excess of 800°C [14].

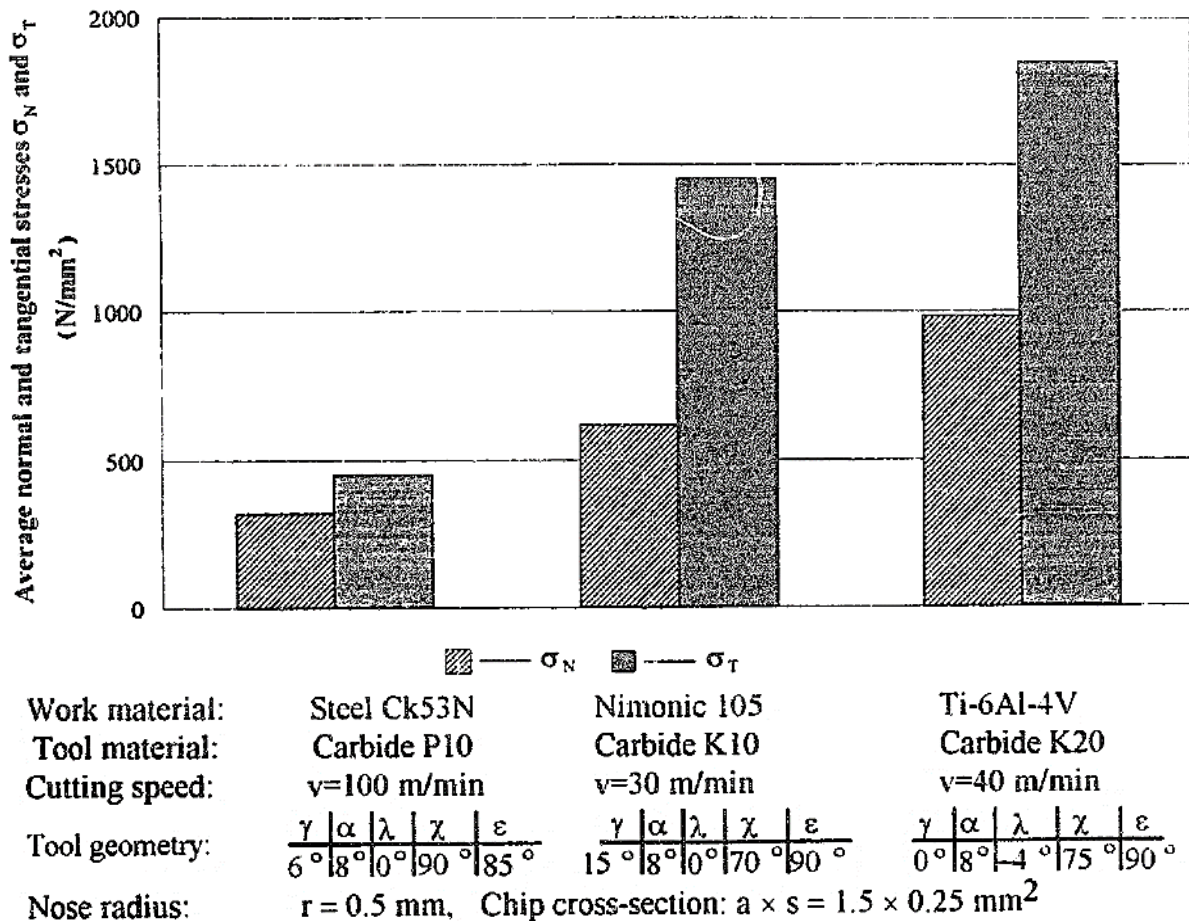


Figure 4 Normal and tangential stresses in machining [14]

2.4.3 Chatter

Chatter is another main problem to be overcome when machining titanium alloys, especially for finish machining, the low elastic modulus of titanium alloys being a principal cause of the chatter during machining. When subjected to cutting pressure, titanium deflects nearly twice as much as carbon steel the greater spring-back behind the cutting edge resulting in premature flank wear, vibration and higher cutting temperature. In effect, there is a bouncing action “as the cutting edge enters the cut. The appearance of chatter may also be partly ascribed to the high dynamic cutting

forces in the machining of titanium. This can be up to 30% of the value of the static forces due to the 'adiabatic or catastrophic thermoplastic shear' process by which titanium chips are formed [14].

2.4.4 Additional criteria for tool materials

Besides high cutting temperatures, high mechanical pressure and high dynamic loads in the machining of titanium alloys, which result in plastic deformation and/or rapid tool wear, cutting tools also suffer from strong the chemical reactivity of titanium. Titanium and its alloys react chemically with almost all tool materials available at cutting temperature in excess of 500°C due to their strong chemical reactivity. The tendency for chips to pressure weld to cutting tools, severe dissolution-diffusion wear, which rises with increasing temperature, and other peculiar characteristics already mentioned, demand additional criteria in the choice of the cutting tool materials.

The chemical composition, mechanical properties and physical properties are given in the table 1, 2 and 3 respectively.

Table 1 Chemical composition of Titanium 6Al4V (wt %)

Material	Ti	V	Al	Cr	Cu	Fe	Mn
Titanium 6Al4V	89.4	4.30	6.15	.0027	.0045	.0510	.0055

Table 2 Mechanical properties of Titanium 6Al-4V

Material	Tensile Strength (MPa)	Yield Strength (MPa)	Poisson's Ratio	Elastic Modulus (GPa)	Shear Modulus (GPa)	Hardness Brinell (HB max)
Titanium 6Al-4V	≥895	≥828	0.31	105-120	41-45	334

Table 3 Physical properties of Titanium 6Al-4V

Material	Density (g/cm ³)	Melting Point (°C)	Thermal Conductivity (W/m.K)	Specific Heat Capacity (J/g.°C)	Co-eff of Thermal Expansion 0-500°C (µm/m.°C)
Titanium 6Al-4V	4.43	1674	6.7	0.5263	9.7

2.5 Micro-milling vs Macro-milling

It seems to be micro-milling is scale down marching operation of macro-milling but there are differences between these processes.

2.5.1 Cutting tool diameter

Diameter of cutting tool used in micro-milling is less than 1 mm while in macro-milling it is greater 1 mm [1, 5, 9, 16, 17].

2.5.2 Tool wear

Tool breaks quickly in micro-milling while in other process tool wears gradually. Fracture of micro tools occur as stresses go beyond the strength of tools due to increase in cutting forces with the blunting of cutting edges [18, 19].

2.5.3 Minimum Chip Thickness

Minimum chip thickness can be described as smallest chip thickness in undeformed condition that is cut stably from a workpiece surface for a specific cutting tool edge radius [5]. In macro-milling depth of cut (a_p) is many times greater than cutting tool edge radius (r_e) and in micro-milling it is close to edge radius of the cutting tool (Fig. 5) [6]. The value of minimum chip thickness usually ranges between 5 % to 38 % of cutting tool edge radius [16]. Fig. 6 shows there are four situations that take place during the process of micro-milling.

1. Rubbing and Burnishing: When depth of cut is smaller than edge radius of the cutting tool or minimum chip thickness either rubbing or burnishing occurs and no chip is formed (Fig. 6a and 6b) [5].
2. Ploughing: If the value of depth of cut reaches close to edge radius of the tool or minimum chip thickness but still less than cutting edge radius of the tool, ploughing starts. Ploughing is phenomenon in which cutting takes place with negative effective rake angle or workpiece slightly deforms due to shearing of material (Fig. 6c) [5, 16].
3. Cutting: When depth of cut becomes greater than edge radius of the cutting tool then there is change of rake angle from negative to positive and actual cutting occurs (Fig. 6d) [5].

Ali et al. suggested that depth of cut is the most important factor to find out minimum chip thickness and to avoid tool fracture [17].

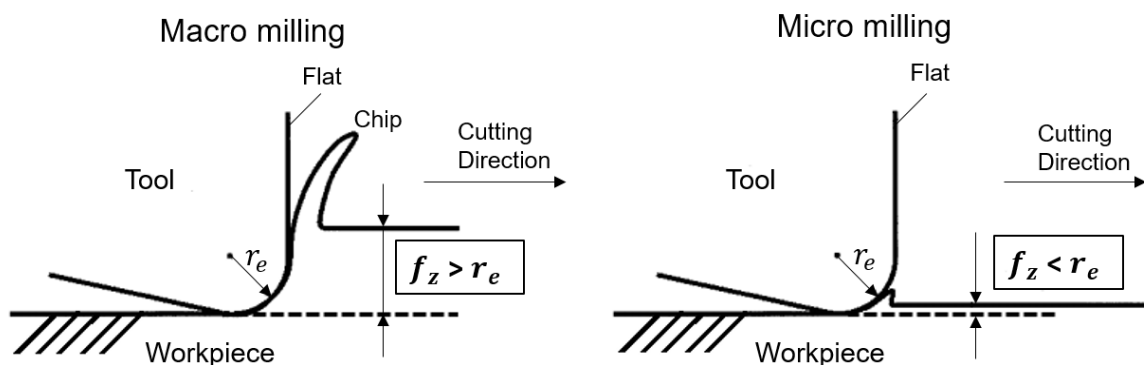


Figure 5 Schematic of macro and micro milling process

2.5.4 Burr Formation

Burr formation is another factor that differentiates micro and macro milling. Lee and Dornfeld et al. found that for micro-milling tool exit and entrance burr was bigger in size than macro milling, considering burr size to chip load ratio. They also explained that tool wear relates with burr height and burr height is proportional to feed. Size effect also plays an important role in burr formation and with the increase in edge radius of the cutting tool larger burrs are produced [20, 21].

Mian et al. conducted micro-milling experiments on AISI 1005 steel and AISI 1045 steel and observed that best surface finish was achieved when feed rate was just close to cutting tool edge radius. He also conducted micro-milling experiment on NiTi alloy and found that feed rate to undeformed minimum chip thickness is the most critical factor in reducing burr root thickness. At high values of chip load cutting starts earlier as compared to low undeformed chip thickness, as a consequence of this ploughing effect becomes less pronounced [1, 22].

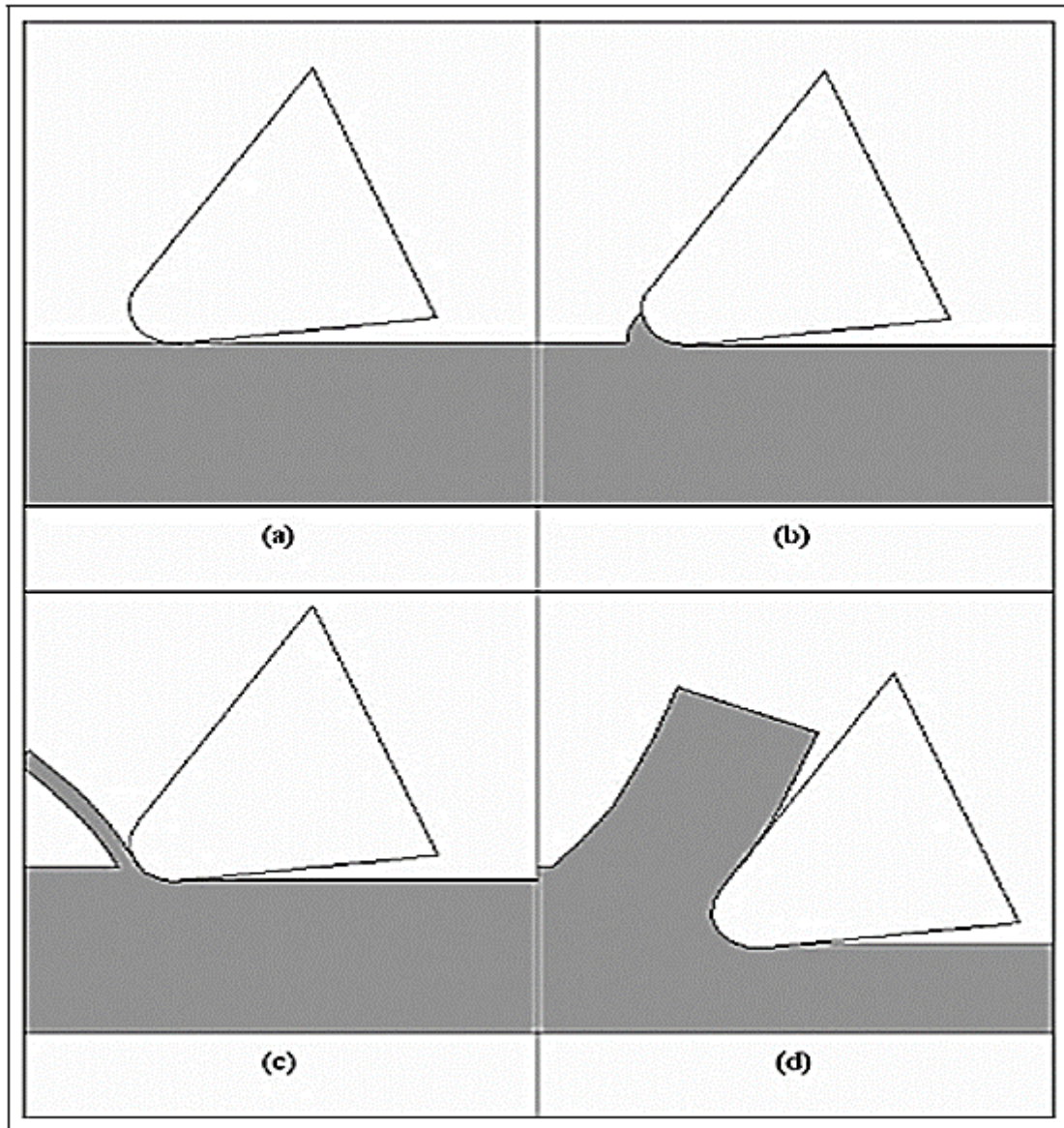


Figure 6 Micro-milling tool workpiece interaction [6]

Kiswanto et al. studied the effect of cutting parameters on surface roughness and burr formation in the micro-milling of Aluminum alloy 1100 and found that surface roughness would increase by increasing feed rate. He further explained different types of burrs and also concluded that; to reduce the burr formation up milling cutting strategy should be used (Fig. 7) [23]. Bajpai et al. performed micro-milling experiments on Titanium 6Al-4V alloy with maximum cutting speed of 90000 RPM and observed that side exit burr is the most critical among all other burr types in up milling. He also found out that increase in chip load, depth of cut and cutting velocity results in improved surface finish [4].

Lekkala et al. analyzed the burr formation in micro-end milling of Aluminum and Steel using experimental and theoretical techniques. He reported that either in down milling or up milling, burr height increases with the decrease in number of flutes and cutting tool diameter and burrs formed in the case of stainless steel were larger than aluminum [24]. Filiz et al. used tungsten carbide micro cutting tools to investigate micro-machinability of copper 101 and found that feed rate is directly proportional to surface roughness and inversely proportional to burr formation and cutting speed is directly proportional to burr formation. At higher feed rates the process is dominated by shearing which results in decrease in burr formation as compared to ploughing [25]. Fang and Liu suggested that after defining cutting and other machine parameters, tool sharpness undeformed chip thickness are the most critical factors to determine burr height [26].

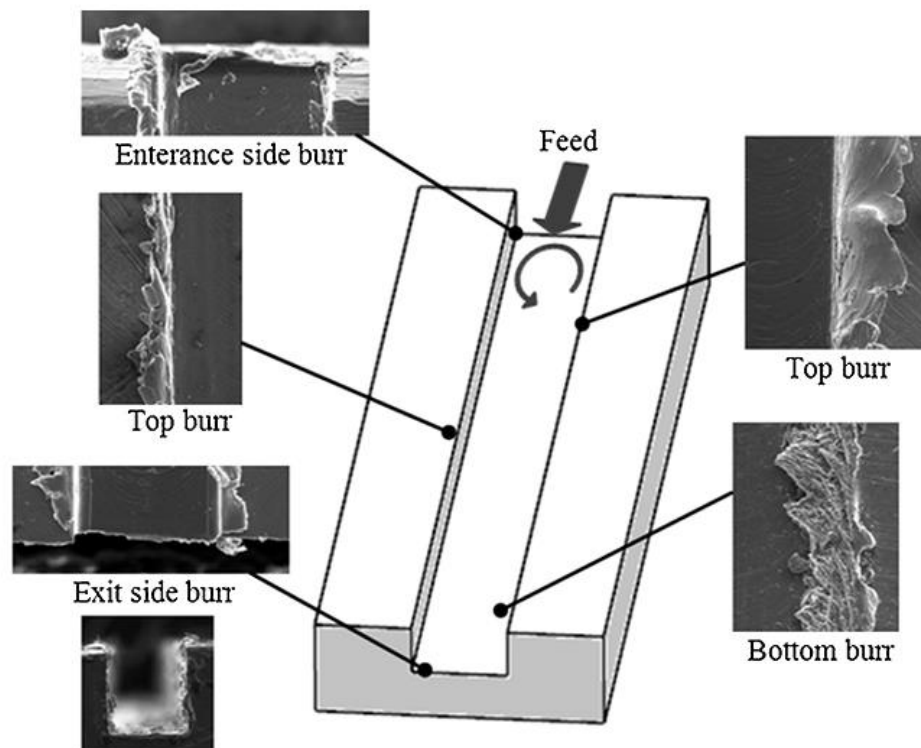


Figure 7 Types of milling Burrs [24]

2.6 Micro-milling Applications

Emerging miniaturization technologies, now-a-days are future key technologies that will introduce totally distinct ways how humans and machines would interact with

the real world. It is likely to be expected that there would be exponential growth in the manufacturing of miniaturized components and their application in the coming years [2].

Micro-milling technology is capable to meet demands of miniaturized components of different fields i.e. aerospace, biomedical, information technology, jewelry, telecommunication industries, automotive, electronics and watch-making.

2.6.1 Biomedical

Moulds for medical components (microdosage systems), moulds for orthodontics (dental brackets), microtools for surgery, moulds for biotechnology applications (microchip electrophoresis devices, polymeric BIOMEMS devices, cataract lenses, accelerating polymerase chain reaction for modular lab-on-a-chip systems), lab-on-chip, retinal micro-tacks, etc.

2.6.2 Information technology

Test membrane for PC chip manufacturing, etc.

2.6.3 Watchmaker and jewelry

Moulds for rings and pendants, manufacturing and engraving of watch base plates, etc.

2.6.4 Automotive

Electrodes for cutting inserts, injection nozzles, etc.

2.6.5 Telecommunications

Multi fibre connector for single and multimode applications, joining elements, mould for easy-assembly etc.

2.6.6 Aerospace

Mould for miniature planetary gear wheels attached to a turbine, miniature devices for rockets and etc.

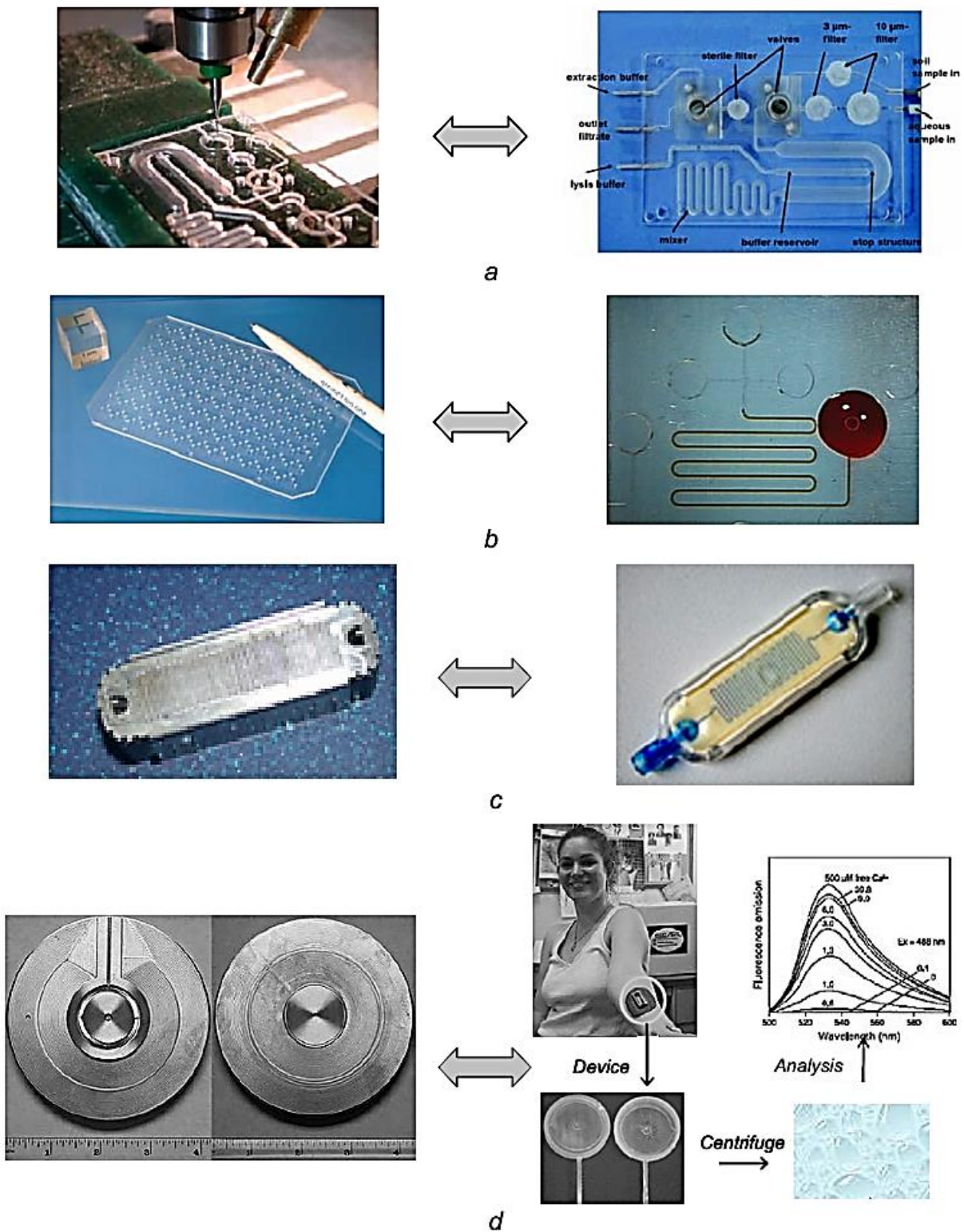


Figure 8 (a) Lab-on-a-chip; (b) Microplate with 96 capillarity electrophoresis system (vacuum hot-embossing plate from micro-milled mould) and filling of one structure; (c) Medicine micro-dosage system; (d) Sweat-stick for collecting human sweat [3]

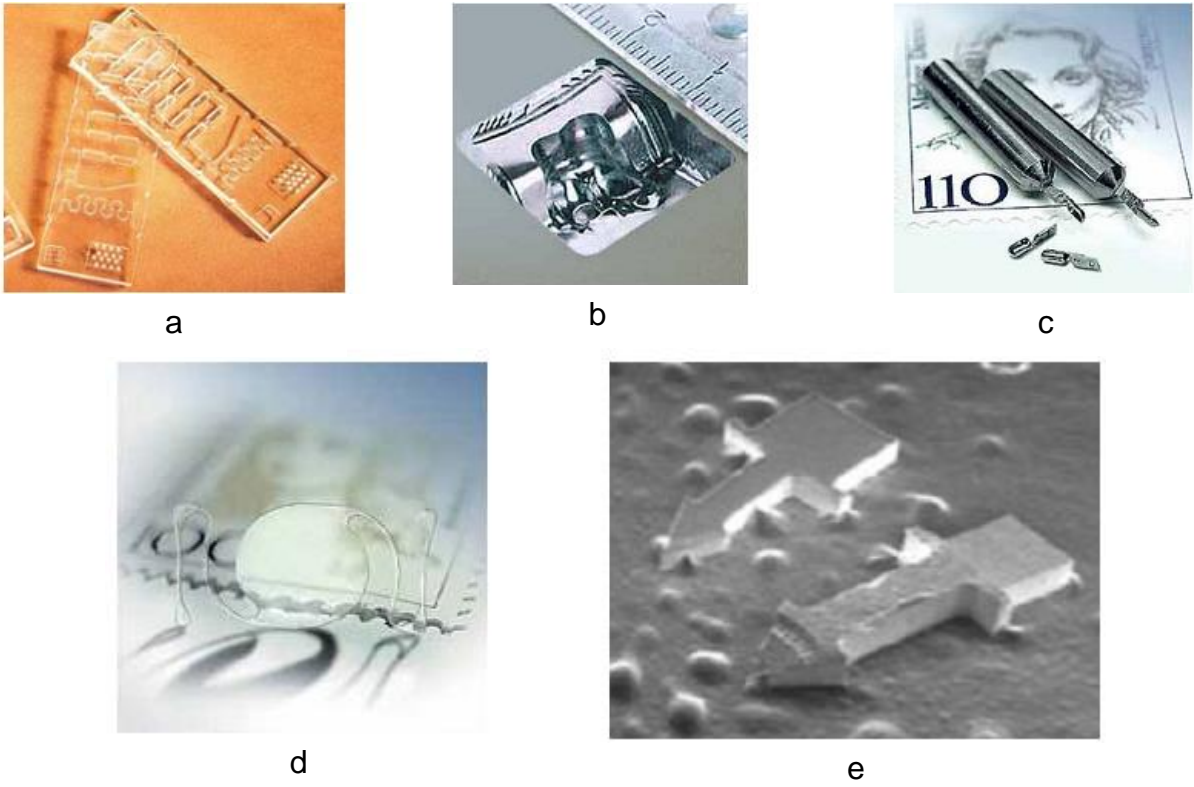


Figure 9 (a) Integrated polymer microfluidic stacks (chemiluminescence experiment); (b) Dental brackets; (c) Tissue removal tools for endoscopy; (d) Cataract lenses; (e) Fabrication of Ti retinal microtack [3]

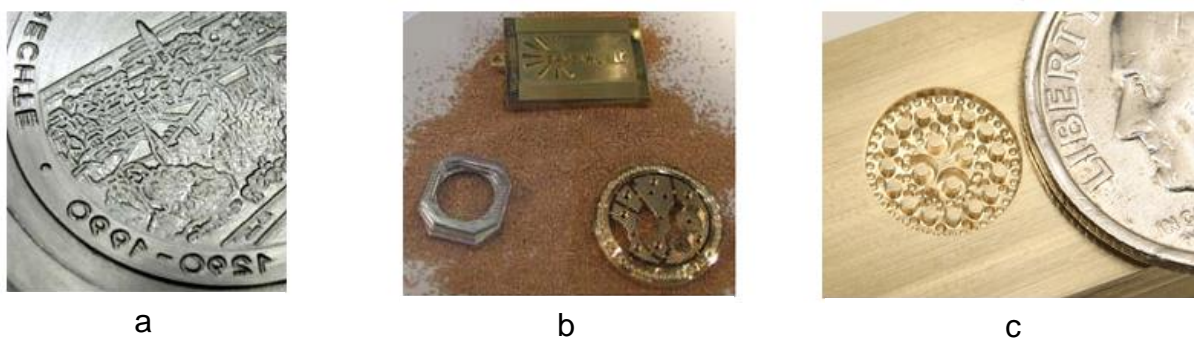


Figure 10 (a) Engraving watch base plate; (b) Watch parts; (c) Pendant mould [3]

2.6.7 Others

Electrodes for manufacturing shaving head of electric razors, electrodes for toy industry, components for measuring devices, etc.

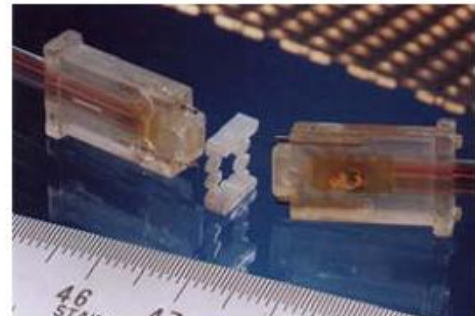
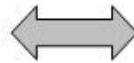
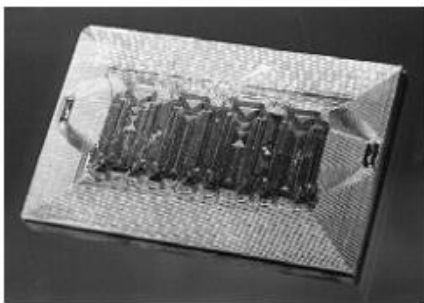


a



b

Figure 11 (a) Injection nozzles for diesel engines; (b) Electrodes for cutting inserts [3]



a

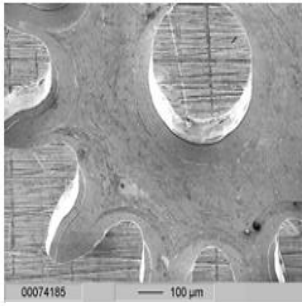


b



c

Figure 12 (a) Multi-fibre connector (micro-milled mould for X-ray mask fabrication and microinjected connector); (b) Joining element for optical fibre connector; (c) Test membrane for computer chip manufacturing [3]



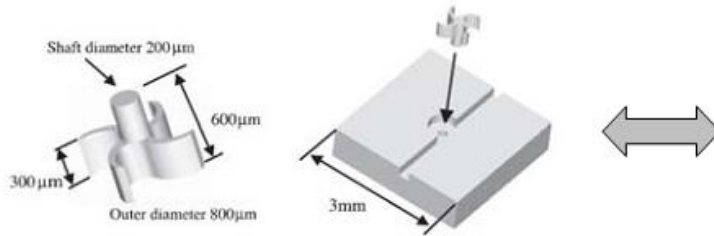
a



b



c



d



Figure 13 (a) Mixing disc of a rocket motor; (b) Turbine wheel for microfluidic pump; (c) Micro-mould of a planetary gear wheel; (d) Assembled micro impeller and base block [3]

METHODOLOGY

Micro-milling experiments were conducted on Titanium Alloy Ti-6Al-4V. The tests were conducted using a FANUC MV-1060 conventional speed machining center. Fig. 14 shows experimental setup. Relative motion between micro end-milling tool and workpiece was controlled by FANUC 0i-MC motion controller.

The tools used during micro-milling experiments of Ti-6Al-4V were ultrafine tungsten carbide tools (North Carbide Tools). The tools used were flat end mills with diameter of 500 μm , helix angle of 30° and number of flutes two. The average tool edge radii of micro-tools were found to be 3.5 μm with standard deviation of 0.5 μm .

The dimensions of the block that was mounted on fixture were 10 x 20 x 10 mm. Full immersion milling was conducted with different axial depth of cuts. Slots of 10 mm in length were machined in each trial to minimize the effect of tool wear on measured data. Three independent runs for each experiment were run to estimate error variance. Experimental conditions are outlined in Table 4.

Table 4 Experimental Conditions

Workpiece	Ti-6Al-4V (Grade 5)
Milling Tool	Two flute Tungsten Carbide micro end mill Tool diameter = 500 μm
Cutting Fluid	Dry Cutting
Length of cut	10 mm
Milling Type	Full immersion

3.1 Experimental Design

Micro-milling experiments were designed based on Taguchi's L9 orthogonal array with three factors and three levels. Three independent factors of feed per tooth, cutting speed and axial depth of cut were considered. Process parameters and level details are given in Table 5.

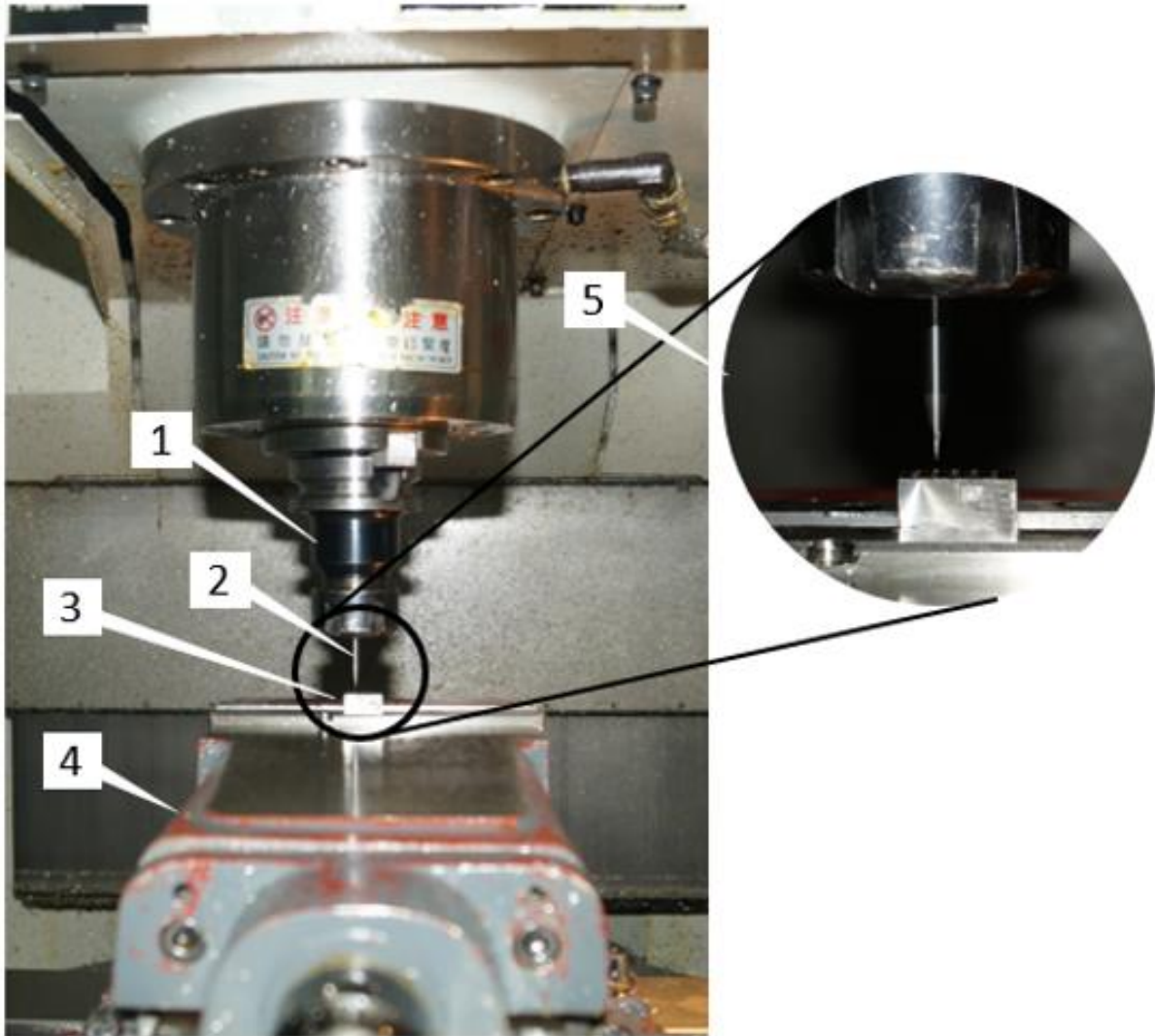


Figure 14 Experimental Setup (1) Spindle; (2) Micro-end mill; (3) Workpiece; (4) Machining vise; (5) Magnified view of tool and workpiece

Table 5 Process Parameters

Process Parameter	Level 1	Level 2	Level 3
f_z ($\mu\text{m}/\text{tooth}$)	8	10	12
V_c (m/min)	5	7.5	10
a_p (μm)	50	75	100

3.2 Selection of Parameters

The levels of feed per tooth, cutting speed and depth of cut (Table 5) have been selected according to the following criteria:

3.2.1 Feed per tooth

Edge radius of the 3 tool was found using scanning electron microscope and average edge radius was measured 3.5 μm with standard deviation of 0.5 μm . Jaffery et al. in his research found that residual effects were more significant when feed per tooth was selected below edge radius [5]. Therefore, in this research to minimize the effect of residual effects feed rate was selected above tool edge radius between 8 and 12 $\mu\text{m}/\text{tooth}$.

3.2.2 Cutting Speed

In literature reported cutting speed varies between 16 m/min (10,000 rpm) and 141 m/min (90,000 rpm) [4]. While this research focuses on machining below the reported minimum cutting speed. Therefore, in this research cutting speed was selected below 16 m/min (10,000 rpm) between 5 m/min (3183 rpm) and 10 m/min (6366 rpm).

3.2.3 Depth of Cut

For every tool, according to its diameter, there is recommended depth of cut to be used. According to Niagara Cutter [27]:

For Tool Diameters 1/8" (3.18 mm) and Under

$a_p = \text{Dia. of Tool} \times (0.25 \text{ to } 0.05)$

Dia of tool used = 0.5 mm

min $a_p = 0.5 \times 0.05 = 0.025 \text{ mm} = 25 \mu\text{m}$

max $a_p = 0.5 \times 0.25 = 0.125 \text{ mm} = 125 \mu\text{m}$

Therefore, in this research depth of cut was selected between 25 – 125 μm . The spindle revolutions per minute (N) and feed speed (V_f) can be determined using the equations (1) and (2) respectively.

$$N = \frac{V_c}{\pi \times D} \quad (1)$$

$$V_f = f \times N \times z \quad (2)$$

Actual values of revolutions per minute and feed speed are listed in Table 6

Table 6 L9 array (RPM and feed speed)

Sr. No.	f_z ($\mu\text{m}/\text{tooth}$)	V_c (m/min)	a_p (μm)	V_f (mm/min)	N (rpm)
1	8	5	50	50.93	3183
2	8	7.5	75	76.39	4774
3	8	10	100	101.85	6366
4	10	5	75	63.66	3183
5	10	7.5	100	95.49	4774
6	10	10	50	127.31	6366
7	12	5	100	76.39	3183
8	12	7.5	50	114.58	4774
9	12	10	75	152.78	6366

3.3 Experimentation

- Experimentation is conducted for worst scenario that is why dry machining condition was used [1].
- For precise and accurate tool offset measurement, multi-meter was used.
- Depending on length of workpiece 3-7 slots were machined on each workpiece keeping a gap of 3 mm between slots and cut length was 10 mm. Figure 13 shows workpiece after machining.

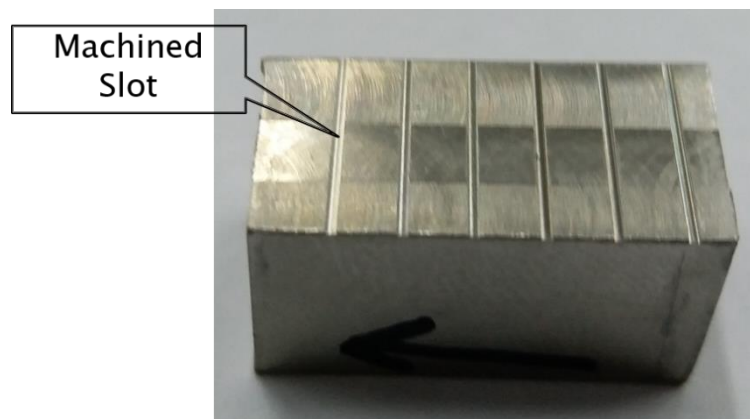


Figure 15 Workpiece after micro-milling

RESULTS AND DISCUSSION

In every experimental run results were obtained in the form of top burr width. Table 7 shows obtained results outlined in the form of L9 array. In micro-milling different types of burrs such as top burr, exit burr, entrance burr and bottom burr are formed depending on direction of cutting and tool workpiece interaction as shown in Fig. 7 [23]. Top burr formation was given special attention which is important burr mechanism during full immersion milling process. Fig. 16 illustrates how top burr width is measured. Top burr can be described as horizontal length of burr from groove wall [10]. Fig. 17 shows burr formation on down milling and up milling side and it can be seen that size of burr is larger at down milling side. The reason for this phenomenon is that velocity of localized cutting edges on the side of up milling side would always be greater than on the side of down milling therefore causing larger burrs to form on down milling side. Similar observations have been reported by Jaffery et al. [5]. Top burr measurement was taken on the side of down milling and it was measured using Scanning Electron Microscope (SEM).

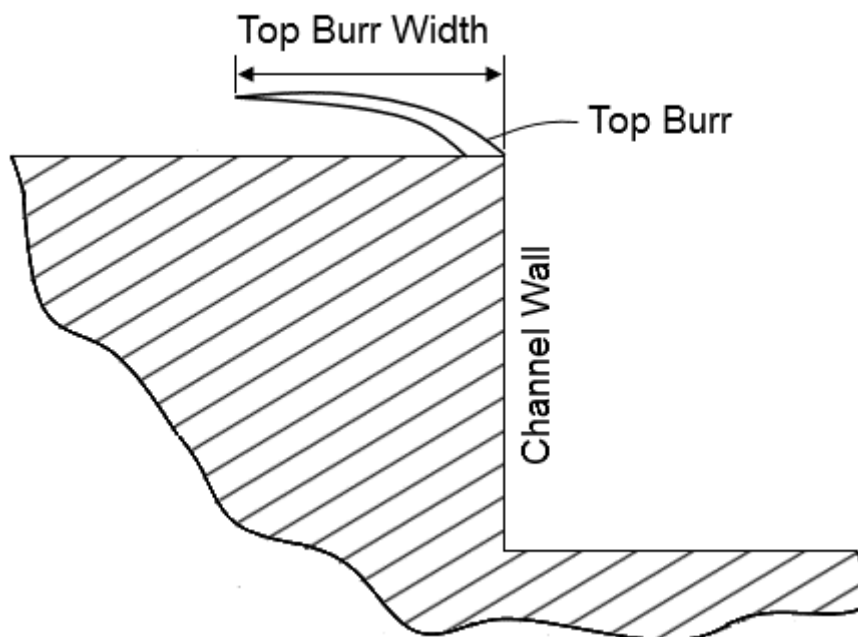


Figure 16 Top burr width measurement

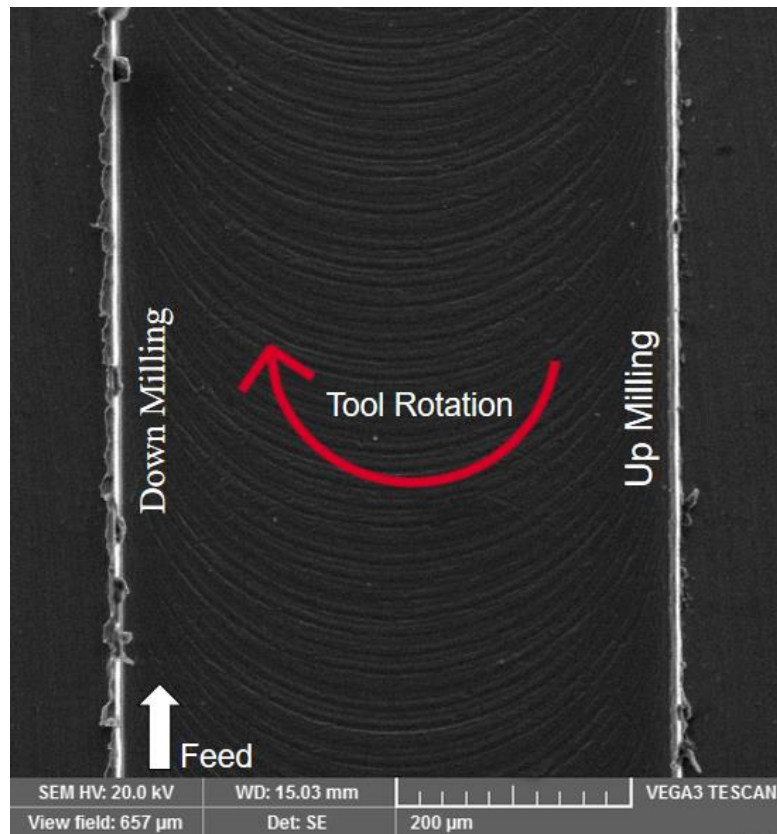


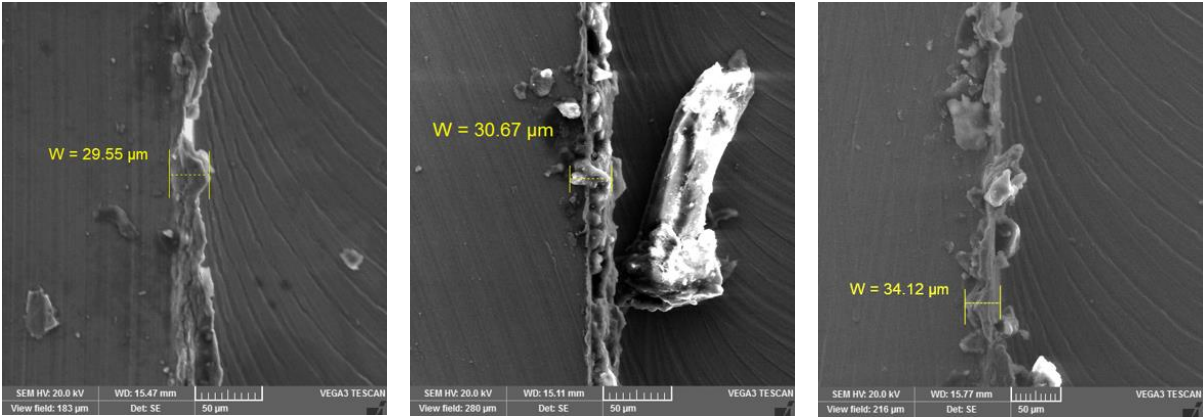
Figure 17 Burr formation at down milling and up milling side

4.1 SEM Images

Fig. 18 shows scanning electron microscope (SEM) utilized to measure the top burr width in the slots.



Figure 18 Scanning Electron Microscope (SEM)

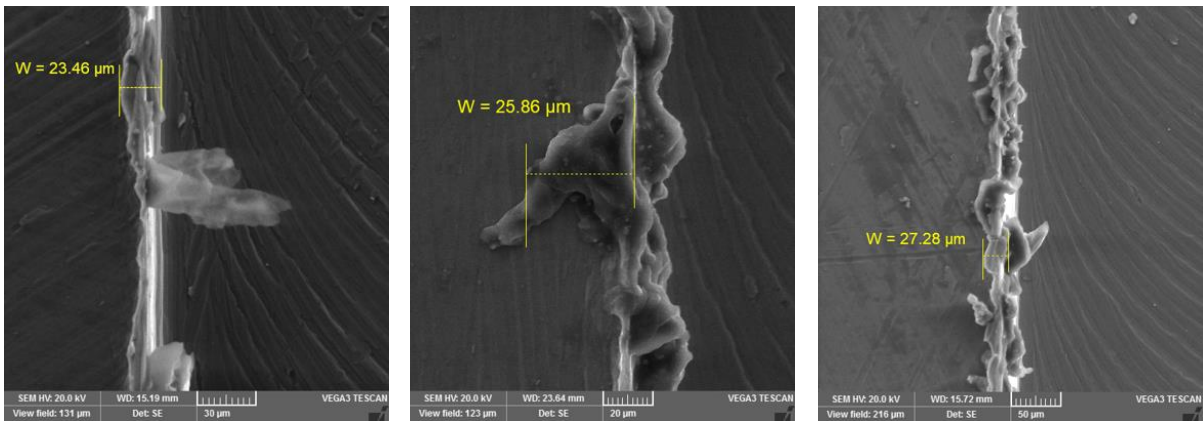


Run 1

Run 2

Run 3

Figure 19 SEM images at $f_z = 8 \mu\text{m/tooth}$, $V_c = 5 \text{ m/min}$, $a_p = 50 \mu\text{m}$

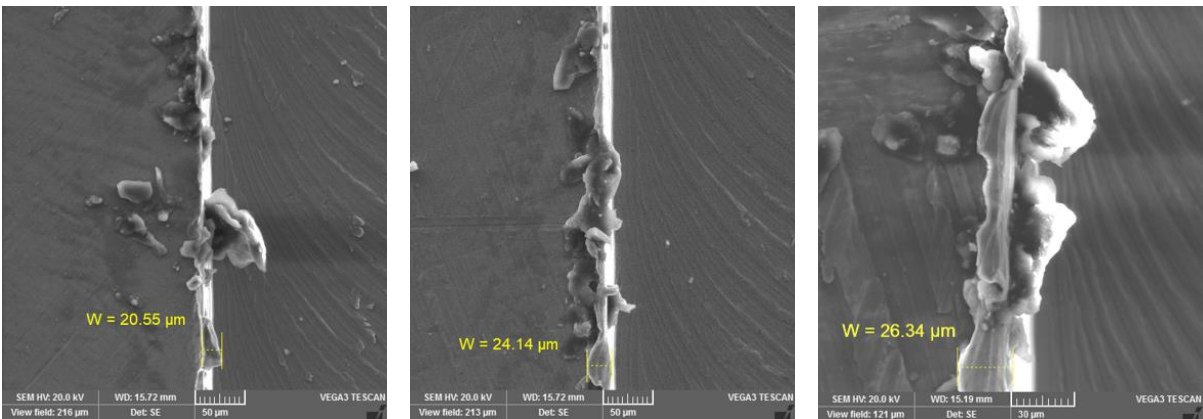


Run 1

Run 2

Run 3

Figure 20 SEM images at $f_z = 8 \mu\text{m/tooth}$, $V_c = 7.5 \text{ m/min}$, $a_p = 75 \mu\text{m}$

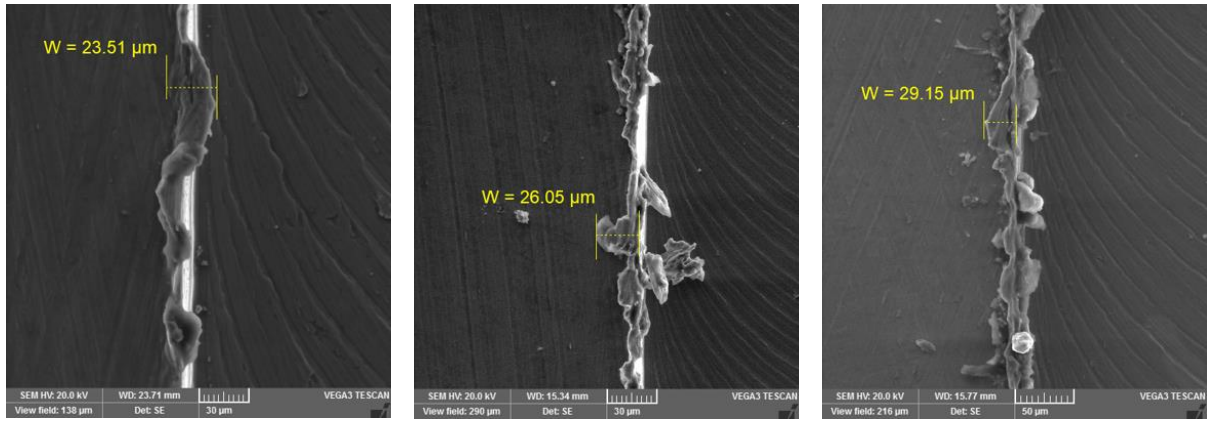


Run 1

Run 2

Run 3

Figure 21 SEM images at $f_z = 8 \mu\text{m/tooth}$, $V_c = 10 \text{ m/min}$, $a_p = 100 \mu\text{m}$

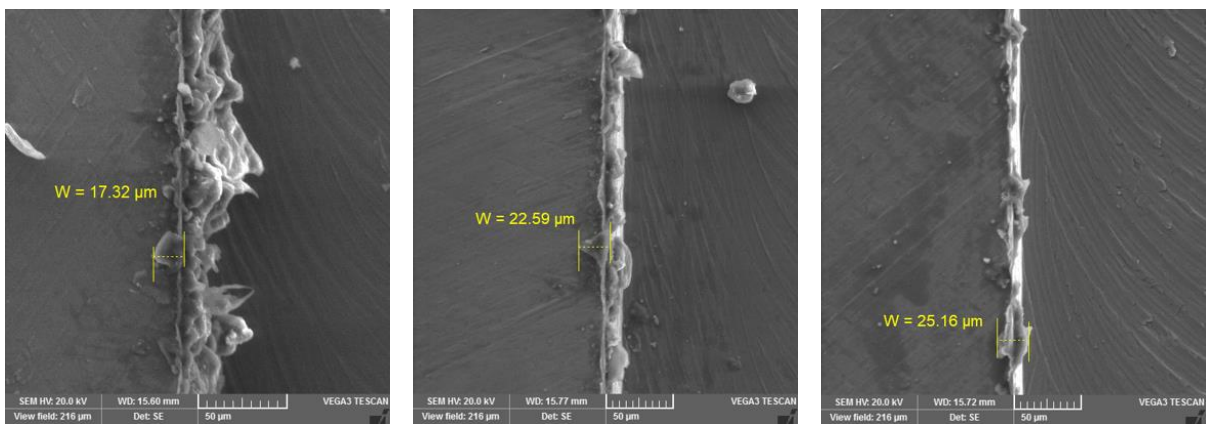


Run 1

Run 2

Run 3

Figure 22 SEM images at $f_z = 10 \mu\text{m/tooth}$, $V_c = 5 \text{ m/min}$, $a_p = 75 \mu\text{m}$

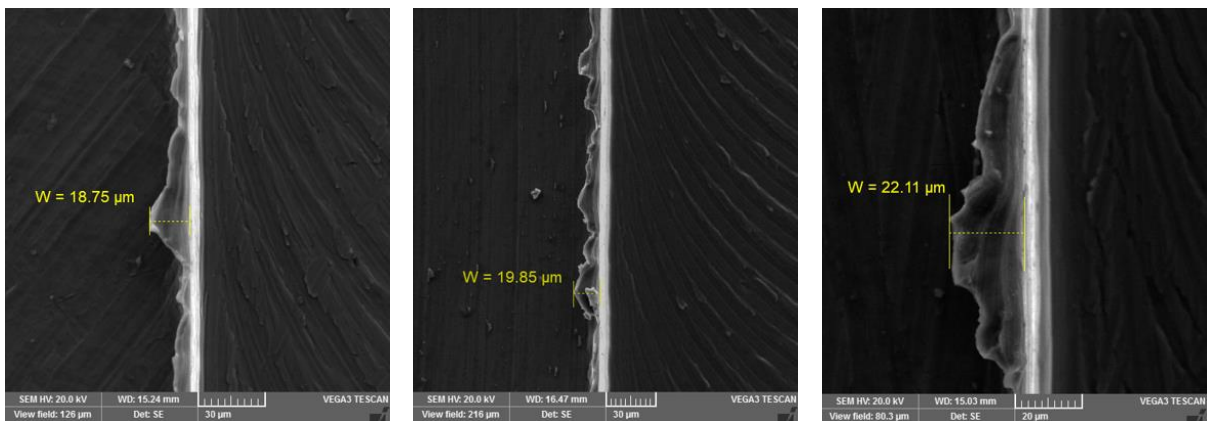


Run 1

Run 2

Run 3

Figure 23 SEM images at $f_z = 10 \mu\text{m/tooth}$, $V_c = 7.5 \text{ m/min}$, $a_p = 100 \mu\text{m}$

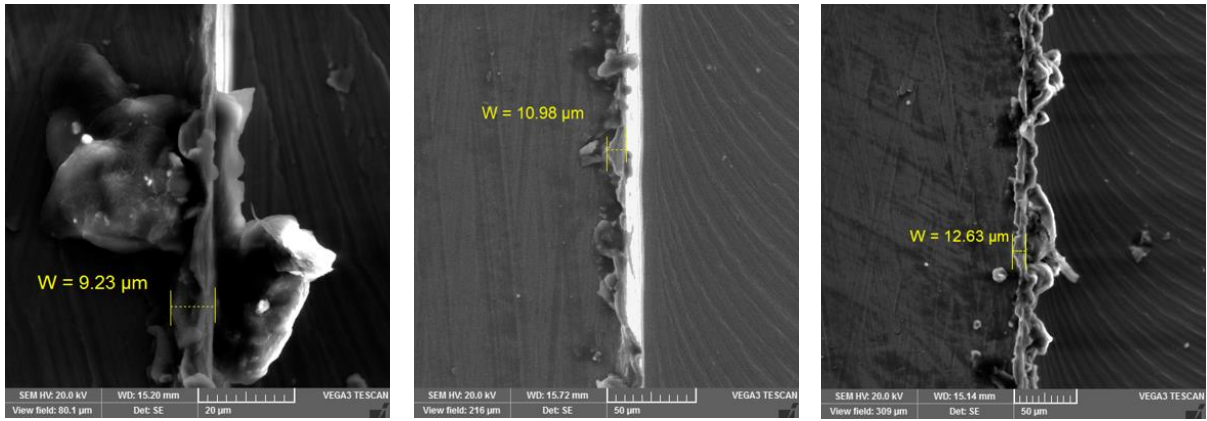


Run 1

Run 2

Run 3

Figure 24 SEM images at $f_z = 10 \mu\text{m/tooth}$, $V_c = 10 \text{ m/min}$, $a_p = 50 \mu\text{m}$

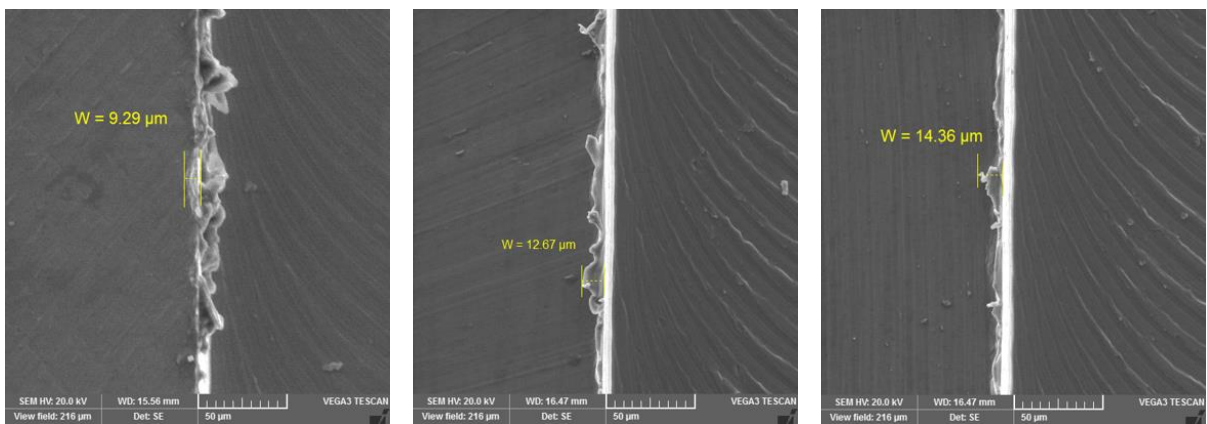


Run 1

Run 2

Run 3

Figure 25 SEM images at $f_z = 12 \mu\text{m/tooth}$, $V_c = 5 \text{ m/min}$, $a_p = 100 \mu\text{m}$

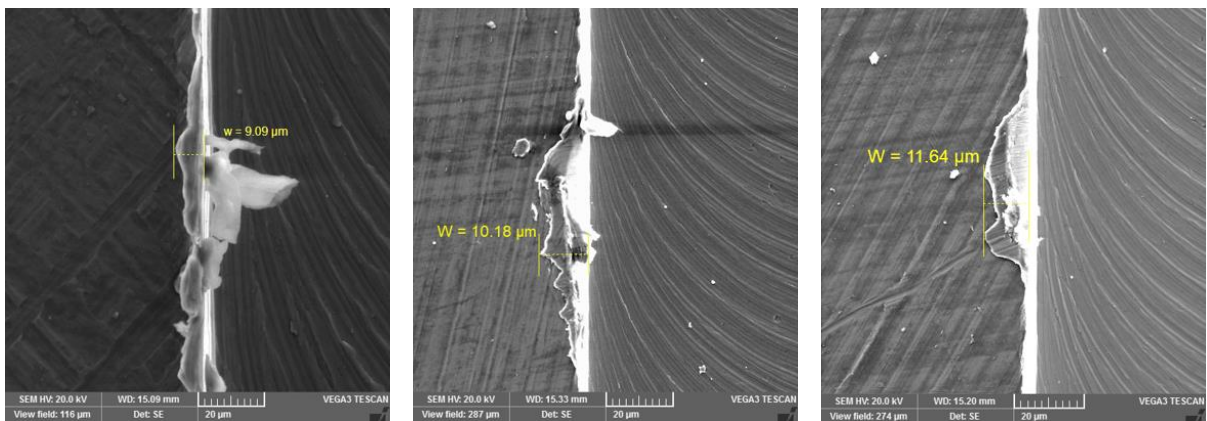


Run 1

Run 2

Run 3

Figure 26 SEM images at $f_z = 12 \mu\text{m/tooth}$, $V_c = 7.5 \text{ m/min}$, $a_p = 50 \mu\text{m}$



Run 1

Run 2

Run 3

Figure 27 SEM images at $f_z = 12 \mu\text{m/tooth}$, $V_c = 10 \text{ m/min}$, $a_p = 75 \mu\text{m}$

Table 7 L9 array (cutting tests with measured outputs)

f_z ($\mu\text{m}/\text{tooth}$)	V_c (m/min)	a_p (μm)	V_f (mm/min)	N (rpm)	Burrs (down-milling side) (μm)		
8	5	50	50.93	3183	29.15	30.67	34.12
8	7.5	75	76.39	4774	23.46	25.86	27.28
8	10	100	101.85	6366	20.55	24.14	26.34
10	5	75	63.66	3183	23.51	26.05	29.15
10	7.5	100	95.49	4774	17.32	22.59	25.16
10	10	50	127.31	6366	18.75	19.85	22.11
12	5	100	76.39	3183	9.23	10.98	12.63
12	7.5	50	114.58	4774	9.29	12.67	14.36
12	10	75	152.78	6366	9.09	10.18	11.64

4.2 ANOVA (Analysis of Variance)

After obtaining results of top burr width using SEM, ANOVA was used for statistical analysis of results. ANOVA is a statistical technique used to assess the significance of process parameters on output responses. To find out impact of each input parameter at output response, sequential sum of squares (SS) was computed using the equation (3) [28].

$$SS_A = \sum_{i=1}^3 \frac{A_i^2}{n} - \frac{(\sum_{j=1}^N T_j)^2}{N} \quad (3)$$

Where A is the process parameter, n is the total number of runs at a particular level, i is the level, T is value of response at each run, j is the number of run, N is the total number of runs. Total sum of squares (SS_T) can be found using equation (4) [28].

$$SS_T = \sum_{j=1}^N T_j^2 - \frac{(\sum_{j=1}^N T_j)^2}{N} \quad (4)$$

Sequential sum of squares of error (SS_e) can be found using equation (5) [28].

$$SS_e = SS_T - \sum_{i=A}^Z SS_i \quad (5)$$

A low value of variance (F-test ratio) for a given parameter shows its low impact on the outcome and vice versa. A p -value is the probability that a test would fail. A p -value less than 0.05 (5%) tells that there are 5% chances that test would fail or 95%

chances that test would succeed. The percentage contribution of each parameter can be computed using equation (6) [28].

$$\%CR = \frac{SS - (df \times MSS_{Res})}{SS_T} \times 100 \quad (6)$$

4.3 ANOVA Calculations

Below are details how sequential sum of square for each parameter is calculated.

4.3.1 Feed per tooth

To calculate sum of squares for *feed per tooth* equation (3) can be written as:

$$SS_A = \frac{(A_1)^2}{n_1} + \frac{(A_2)^2}{n_2} + \frac{(A_3)^2}{n_3} - \frac{(T_1 + T_2 + \dots + T_{27})^2}{N} \quad (7)$$

Using Table 7 as:

	f_z ($\mu\text{m}/\text{tooth}$)	V_c (m/min)	a_p (μm)	Burrs (down-milling side) (μm)			
Level 1	8	5	50	29.15	30.67	34.12	A1
	8	7.5	75	23.46	25.86	27.28	
	8	10	100	20.55	24.14	26.34	
Level 2	10	5	75	23.51	26.05	29.15	A2
	10	7.5	100	17.32	22.59	25.16	
	10	10	50	18.75	19.85	22.11	
Level 3	12	5	100	9.23	10.98	12.63	A3
	12	7.5	50	9.29	12.67	14.36	
	12	10	75	9.09	10.18	11.64	

$$\frac{(A_1)^2}{n_1} = \frac{(29.15+30.67+34.12+23.46+25.86+27.28+20.55+24.14+26.34)^2}{9}$$

$$\frac{(A_1)^2}{n_1} = 6484.01 \quad (a)$$

$$\frac{(A_2)^2}{n_2} = \frac{(23.51+26.05+29.15+17.32+22.59+25.16+18.75+19.85+22.11)^2}{9}$$

$$\frac{(A_2)^2}{n_2} = 4646.24 \quad (b)$$

$$\frac{(A_3)^2}{n_3} = \frac{(9.23+10.98+12.63+9.29+12.67+14.36+9.09+10.18+11.64)^2}{9}$$

$$\frac{(A_3)^2}{n_3} = 1112.67 \quad (c)$$

$$\frac{(T_1+T_2+\dots+T_{27})^2}{N} = \frac{(546.13)^2}{27} = \frac{298257.98}{27} = 11046.59 \quad (d)$$

Putting values from (a), (b), (c) and (d) into equation (7)

$$SS_A = 6484.01 + 4646.24 + 1112.67 - 11046.59 = 1196.32 \quad (A)$$

4.3.2 Cutting Speed

To calculate sum of squares for *cutting speed* equation (3) can be written as:

$$SS_B = \frac{(B_1)^2}{n_1} + \frac{(B_2)^2}{n_2} + \frac{(B)^2}{n_3} - \frac{(T_1+T_2+\dots+T_{27})^2}{N} \quad (8)$$

Using Table 7 as:

	f_z ($\mu\text{m}/\text{tooth}$)	V_c (m/min)	a_p (μm)	Burrs (down-milling side) (μm)		
Level 1	8	5	50	29.15	30.67	34.12
	10	5	75	23.51	26.05	29.15
Level 2	12	5	100	9.23	10.98	12.63
	8	7.5	75	23.46	25.86	27.28
	10	7.5	100	17.32	22.59	25.16
Level 3	12	7.5	50	9.29	12.67	14.36
	12	10	100	20.55	24.14	26.34
	12	10	50	18.75	19.85	22.11
	12	10	75	9.09	10.18	11.64

$$\frac{(B_1)^2}{n_1} = \frac{(29.15+30.67+34.12+23.51+26.05+29.15+9.23+10.98+12.63)^2}{9}$$

$$\frac{(B_1)^2}{n_1} = 4691.79 \quad (e)$$

$$\frac{(B_2)^2}{n_2} = \frac{(23.46+25.86+27.28+17.32+22.59+25.16+9.29+12.67+14.36)^2}{9}$$

$$\frac{(B_2)^2}{n_2} = 3520.05 \quad (f)$$

$$\frac{(B_3)^2}{n_3} = \frac{(20.55+24.14+26.34+18.75+19.85+22.11+9.09+10.18+11.64)^2}{9}$$

$$\frac{(B_3)^2}{n_3} = 2939.45 \quad (g)$$

Putting values from (d), (e), (f) and (g) into equation (8)

$$SS_B = 4691.79 + 3520.05 + 2939.45 - 11046.59 = 104.70 \quad (B)$$

4.3.3 Depth of cut

To calculate sum of squares for *depth of cut* equation (3) can be written as:

$$SS_C = \frac{(C_1)^2}{n_1} + \frac{(C_2)^2}{n_2} + \frac{(C)^2}{n_3} - \frac{(T_1+T_2+\dots+T_{27})^2}{N} \quad (9)$$

Using Table 7 as:

	f_z ($\mu\text{m}/\text{tooth}$)	V_c (m/min)	a_p (μm)	Burrs (down-milling side) (μm)		
Level 1	8	5	50	29.15	30.67	34.12
	12	7.5	50	9.29	12.67	14.36
Level 2	10	10	50	18.75	19.85	22.11
	10	5	75	23.51	26.05	29.15
Level 3	8	7.5	75	23.46	25.86	27.28
	12	10	75	9.09	10.18	11.64
	12	5	100	9.23	10.98	12.63
	10	7.5	100	17.32	22.59	25.16
	8	10	100	20.55	24.14	26.34

$$\frac{(C_1)^2}{n_1} = \frac{(29.15+30.67+34.12+9.29+12.67+14.36+18.75+19.85+22.11)^2}{9}$$

$$\frac{(C_1)^2}{n_1} = 4052.17 \quad (h)$$

$$\frac{(C_2)^2}{n_2} = \frac{(23.51+26.05+29.15+23.46+25.86+27.28+9.09+10.18+11.64)^2}{9}$$

$$\frac{(C_2)^2}{n_2} = 3853.10 \quad (i)$$

$$\frac{(C_3)^2}{n_3} = \frac{(9.23+10.98+12.63+17.32+22.59+25.16+20.55+24.14+26.34)^2}{9}$$

$$\frac{(C_3)^2}{n_3} = 3171.19 \quad (j)$$

Putting values from (d), (h), (i) and (j) into equation (9)

$$SS_C = 4052.17 + 3853.10 + 3171.19 - 11046.59 = 29.87 \quad (C)$$

4.3.4 Error sum of squares

SS_T and SS_e can be found using equation (4) and (5) respectively.

$$SS_T = (T_1)^2 + (T_2)^2 + \dots + (T_{27})^2 - \frac{(T_1+T_2+\dots+T_{27})^2}{N}$$

$$SS_T = 12515.55 - \frac{298257.98}{27} = 1468.96 \quad (D)$$

$$SS_e = SS_T - SS_A - SS_B - SS_C$$

$$SS_e = 1468.96 - 1196.32 - 104.70 - 29.87 = 138.07 \quad (E)$$

4.3.5 Contribution ratio

Contribution ratio of each parameter can be found using equation 6

$$\%CR (feed) = \frac{1196.32 - (2 \times 6.90)}{1468.96} \times 100 = 81\% \quad (F)$$

$$\%CR (speed) = \frac{104.70 - (2 \times 6.90)}{1468.96} \times 100 = 6\% \quad (G)$$

$$\%CR (depth of cut) = \frac{29.87 - (2 \times 6.90)}{1468.96} \times 100 = 1\% \quad (H)$$

$$\%CR (error) = 100 - \%CR (feed) - \%CR (speed) - \%CR (doc)$$

$$\%CR (error) = 100 - 81 - 6 - 1 = 12\% \quad (I)$$

Table 8 ANOVA table (top burr width)

Source	df	SS	MSS = SS/df	F-ratio	p-value	Significance	CR (%)
f_z ($\mu\text{m}/\text{tooth}$)	2	1196.32	598.16	86.64	<0.0010	Significant	81
V_c (m/min)	2	104.70	52.35	7.58	0.0040	Significant	6
a_p (μm)	2	29.87	14.93	2.16	0.1410	Non-significant	1
Res	20	138.07	6.90				12
Total		1468.96					100

df: degree of freedom; SS: sum of squares; MSS: mean sum of squares; CR: contribution ratio

4.3 Burr Formation Analysis

Manual handling of micro-components is not as easy as macro-components. Therefore removal of burr is very difficult and deburring is a process which can be used for removal of burr but it would change part dimensions and its features which is undesirable [1]. ANOVA was carried out to measure impact of parameters on burr width. Burr size was larger on the side of down milling (Fig. 17) so to consider worst case situation burr width was measured on the side of down milling only.

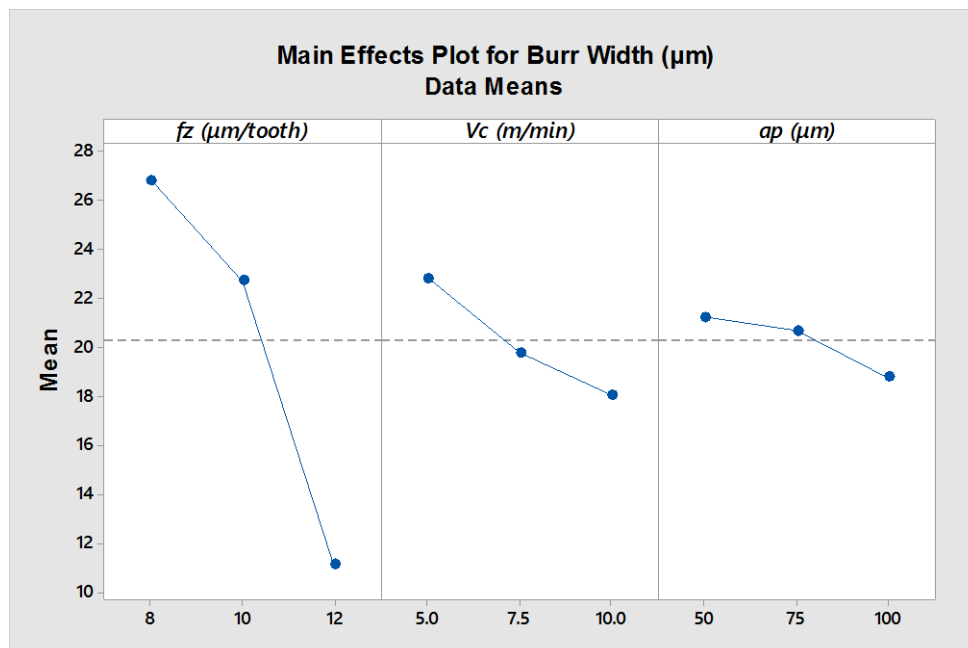


Figure 28 Main effect plots for top burr width with respect to process variables

From Table 8 it can be seen that feed per tooth is the most significant factor contributing 81% causing top burr and cutting speed is another parameter that is

significant with contribution ratio of 6% which shows that it has almost 93% less impact on top burr as compared to feed per tooth. The main effect plots for top burr width were generated using Minitab software (Fig. 28).

Each point in the plot shows mean or average top burr width for a particular level of feed per tooth, cutting speed and depth of cut. The CRs are in consonance with a previous study in which similar analysis was performed on micro-machining of Titanium 6Al-4V alloy [5].

From Fig. 28, it can be seen that top burr width decreases with the increase in feed per tooth. Previous studies reported similar outcomes where researchers found inverse relationship between feed rate and burr formation and concluded that feed per tooth is the most significant parameter influencing top burr formation [3, 11].

The ratio of feed per tooth to edge radius of the cutting tool (f_z/r_e) is also very important in determining process performance [22]. Fig. 29 shows the main effect plot created between f_z/r_e ratio and top burr width. Fig. 30 shows main effect plot created between f_z/r_e ratio and top burr width using data from Jaffery et al. [5].

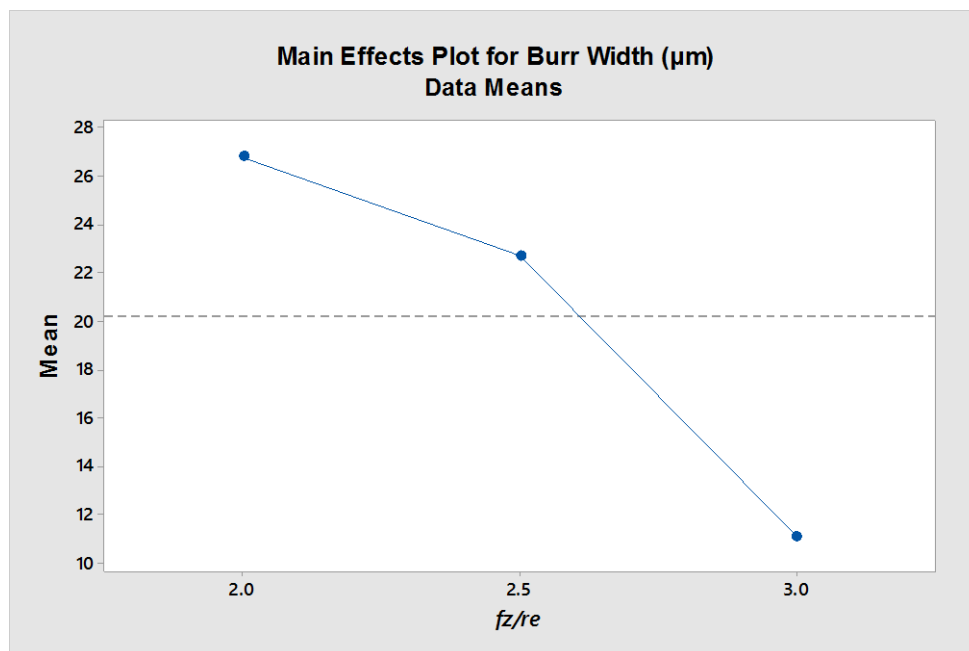


Figure 29 Main effect plot between f_z/r_e and top burr width [5]

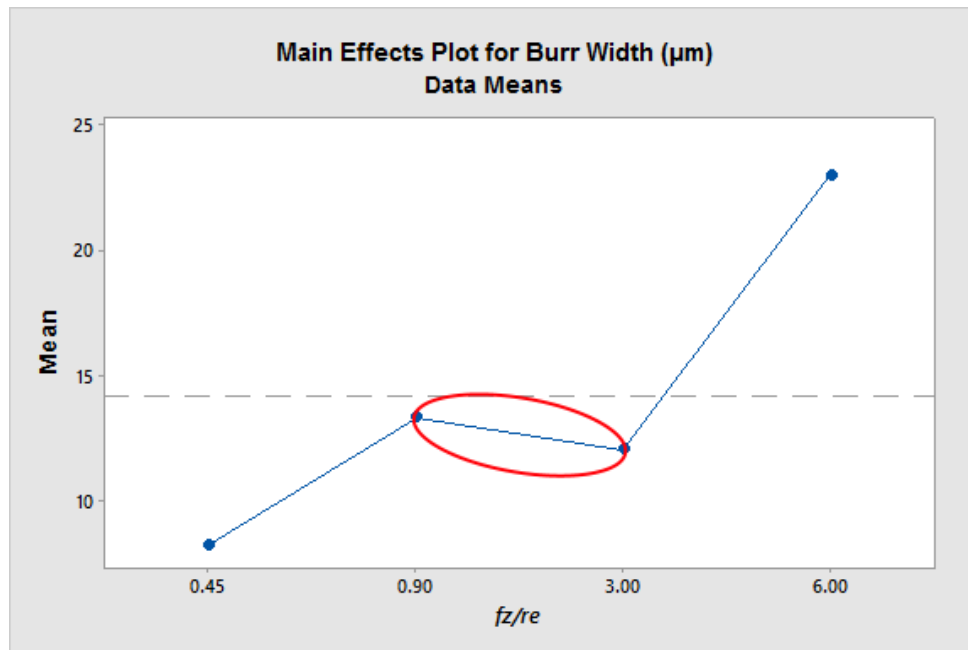


Figure 30 Main effect plot between f_z/r_e and top burr width [6]

By comparing Fig. 29 and Fig. 30 it can be concluded that trend of burr formation with respect to feed rate is in conformance with the research conducted by Jaffery et al. [5]. The region of f_z/r_e (2.0 to 3.0) from Fig. 29 lies within the region of Fig. 30 (0.9 to 3.0).

Main effect plots for cutting speed and depth of cut show a downward trend which means increase in cutting speed and depth of cut reduces the burr width. These result are in conformance with the findings of previous researchers who did similar analysis and experiments on Ti-6Al-4V [3–5, 11]. Since at low cutting speeds frictional force between rake face of the tool and chip is high which can lead to welding phenomenon. Due to welding phenomenon, chips may remain attached to the surface of workpiece in the form of burrs. In the case of depth of cut, at high depth of cut surface temperature decreases and most of the heat generated goes into the chips. To absorb more heat larger chips are produced which ultimately results into less burr formation [29].

4.4 Confirmation test

From main effect plot it is evident that setting feed per tooth, cutting speed and depth of cut at high levels yielded minimum top burr width. Taguchi design of experiment (DOE) is used reduce to number of experiments. Therefore, to ensure

repeatability of the process, a validation experiment is necessary to check the minimization or maximization of the results coming from the optimization process. A confirmation test was carried out for top burr width against the levels of optimal process parameters. A summary of machining conditions and experimental results is given in the Table 9.

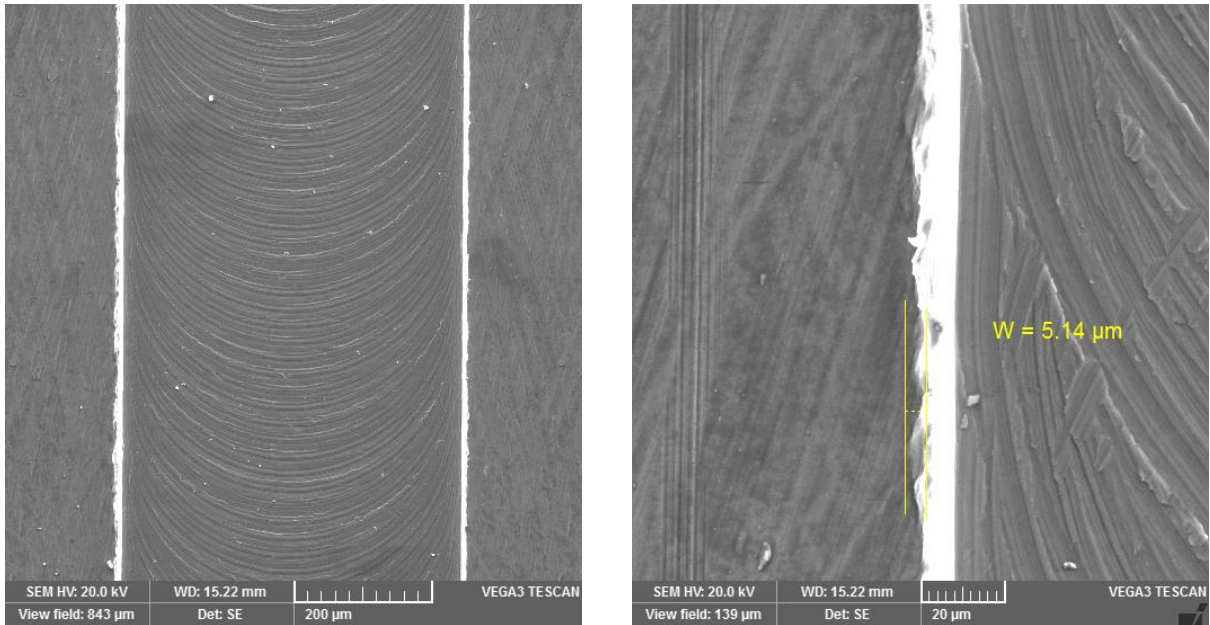
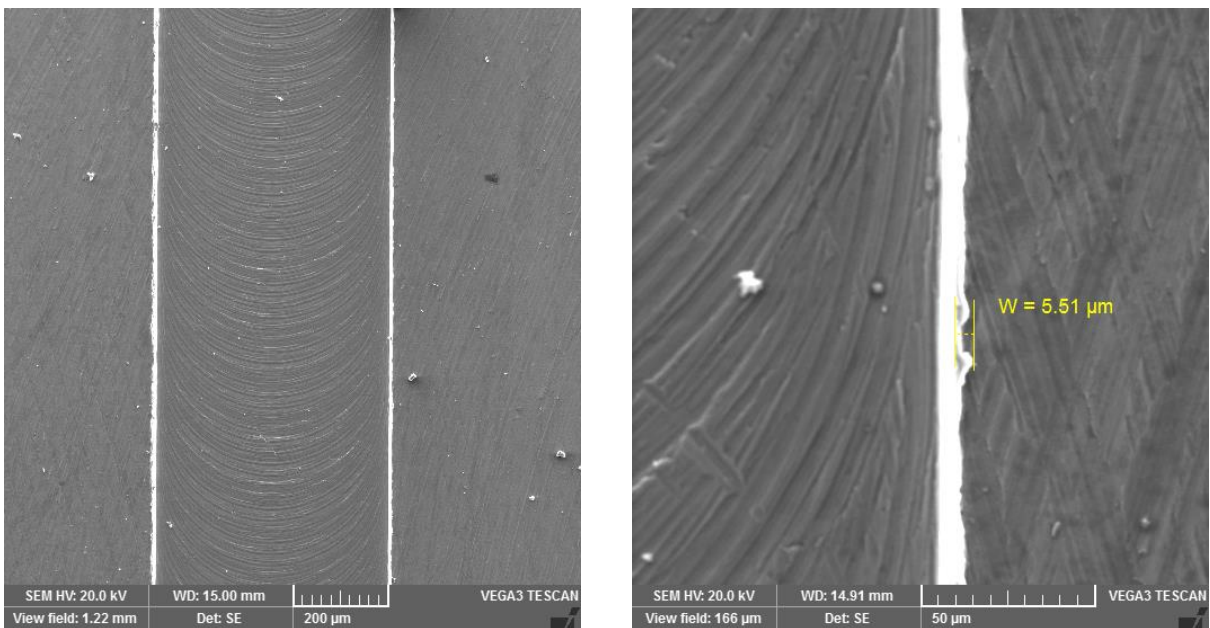
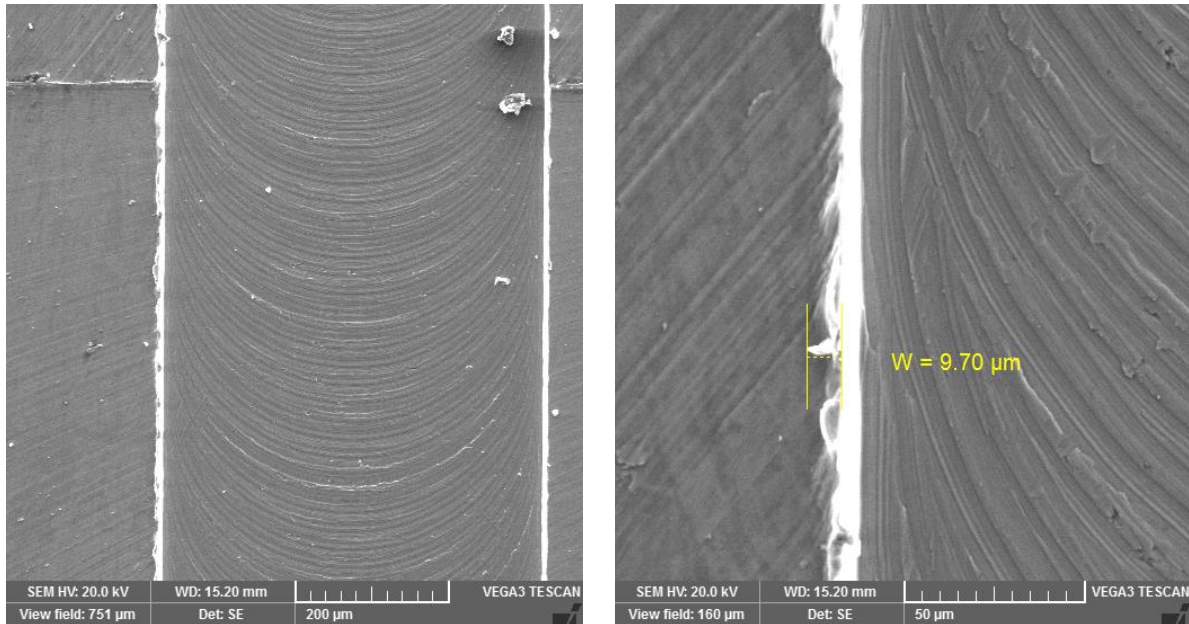


Figure 31 Scanning Electron Microscope image at optimum conditions (Run 1)



Run 2

Figure 32 Scanning Electron Microscope image at optimum conditions (Run 2)



Run 3

Figure 33 Scanning Electron Microscope image at optimum conditions (Run 3)

It is evident from presented results that optimum conditions yield best results as compared to the initial results reported in Table 7. Figs. 31, 32 and 33 shows negligible burr at optimum conditions.

Table 9 Experimental results at optimum conditions

Objective Function	Optimal Process Parameters			Experimental Results	
	f_z ($\mu\text{m}/\text{tooth}$)	V_c (m/min)	a_p (μm)	Top burr width (μm)	
				Ave.	error
Minimum top burr width	12	10	100	6.78	2.53
Maximum top burr width	8	5	50	31.33	2.55

CONCLUSIONS

Identifying KPVs is very important to enhance product quality and at the same time productivity which ultimately leads to reduction in manufacturing costs. The impact of machining parameters in micro-milling is not as same as in macro-machining. This is due to fact that feed rate is almost of the same order as edge radius of the cutting tool. In this paper, KPVs (feed per tooth, cutting speed and depth of cut) were varied to study their effect on burr formation in detail. ANOVA technique was applied on measured outputs to investigate the main effect of cutting parameters on burr formation.

- Machining at optimum conditions gave best outcome in the form of minimum burr on the edges of slot.
- It is clearly evident that to reduce burr formation in micro milling of Ti-6Al-4V instead of using high speed machining setup, low speed machining setup can be used with variation in feed per tooth and better results can be achieved.
- The top burr on the edges of machined slot shows that larger burrs are formed on down milling side.
- At 95% confidence level, feed rate was found to be the most significant factor contributing towards burr formation with contribution ratio of 81%.
- Other than feed per tooth, cutting speed is another control factor affecting burr formation during micro-milling process whose contribution was found to be 6% which is almost 93% less than feed rate contribution.

5.1 Recommendations

- Analysis of surface roughness, tool wear in low speed micro milling of Ti-6Al-4V.
- Analysis of coated and uncoated tools in low speed micro-milling of Ti-6Al-4V with respect to surface roughness, tool wear and burr formation.
- Analysis of subsurface damage in low speed and high speed micro-milling of Ti-6Al-4V.

- Analysis of effect of different coated tools over subsurface damage, tool wear, burr formation and surface roughness in low speed and high speed micro-milling of Ti-6Al-4V.
- Experiment and FEM simulations using coated and uncoated tools with respect to burr formation, surface roughness, tool wear and subsurface damage.

REFERENCES

- [1] Mian AJ, Driver N, Mativenga PT. A comparative study of material phase effects on micro-machinability of multiphase materials. *Int J Adv Manuf Technol* 2010; 50: 163–174.
- [2] University M. MICROMILLING TECHNOLOGY: Global review. <http://www.academia.edu/12679877/Micromilling> (2015, accessed 8 December 2016).
- [3] Kim DH, Lee P-H, Lee SW. Experimental Study on Machinability of Ti-6Al-4V in Micro End-Milling. *Proc World Congr Eng* 2014; II: 0–4.
- [4] Bajpai V, Kushwaha AK, Singh RK. Burr Formation and Surface Quality in High Speed Micromilling of Titanium Alloy (Ti6Al4V). In: *Volume 2: Systems; Micro and Nano Technologies; Sustainable Manufacturing*. ASME, p. V002T03A017.
- [5] Jaffery SHI, Khan M, Ali L, et al. Statistical analysis of process parameters in micromachining of Ti-6Al-4V alloy. *Proc Inst Mech Eng Part B J Eng Manuf*. Epub ahead of print 2015. DOI: 10.1177/0954405414564409.
- [6] Chae J, Park SS, Freiheit T. Investigation of micro-cutting operations. *Int J Mach Tools Manuf* 2006; 46: 313–332.
- [7] Kuram E, Ozcelik B. Multi-objective optimization using Taguchi based grey relational analysis for micro-milling of Al 7075 material with ball nose end mill. *Meas J Int Meas Confed* 2013; 46: 1849–1864.
- [8] Uzun İrfan, Aslantas K, Bedir F. An experimental investigation of the effect of coating material on tool wear in micro milling of Inconel 718 super alloy. *Wear* 2013; 300: 8–19.
- [9] Özel T, Thepsonthi T, Ulutan D, et al. Experiments and finite element simulations on micro-milling of Ti-6Al-4V alloy with uncoated and cBN coated micro-tools. *CIRP Ann - Manuf Technol* 2011; 60: 85–88.

- [10] Thepsonthi T, Özel T. Multi-objective process optimization for micro-end milling of Ti-6Al-4V titanium alloy. *Int J Adv Manuf Technol* 2012; 63: 903–914.
- [11] Thepsonthi T, Özel T. Experimental and finite element simulation based investigations on micro-milling Ti-6Al-4V titanium alloy: Effects of cBN coating on tool wear. *J Mater Process Technol* 2013; 213: 532–542.
- [12] Dynamet Holdings Inc. Technical Datasheet Titanium Alloy Ti 6Al-4V. *Carpenter Technology Corporation* 2015; 1–10.
- [13] Mhamdi M-B, Boujelbene M, Bayraktar E, et al. Surface Integrity of Titanium Alloy Ti-6Al-4V in Ball end Milling. *Phys Procedia* 2012; 25: 355–362.
- [14] Ezugwu EO, Wang ZM. Titanium alloys and their machinability. *J Mater Process Technol* 1997; 68: 262–274.
- [15] Jaffery SI, Mativenga PT. Assessment of the machinability of Ti-6Al-4V alloy using the wear map approach. *Int J Adv Manuf Technol* 2009; 40: 687–696.
- [16] Ducobu F, Filippi E, Rivière-Lorphèvre. Chip Formation and Minimum Chip Thickness in Micro-milling. *Proc 12th CIRP Conf Model Mach Oper* 2009; 1: 339–346.
- [17] Ali MY, Khan AA, Banu A, et al. Prediction of Minimum Chip Thickness in Tool Based Micro End Milling. *Int J Integr Eng* 2012; 4: 6–10.
- [18] Tansel I, Rodriguez O, Trujillo M, et al. Micro-end-milling—I. Wear and breakage. *Int J Mach Tools Manuf* 1998; 38: 1419–1436.
- [19] Tansel I., Arkan T., Bao W., et al. Tool wear estimation in micro-machining. *Int J Mach Tools Manuf* 2000; 40: 599–608.
- [20] Lee K, Dornfeld DA. An Experimental Study on Burr Formation in Micro Milling Aluminum and Copper. In: *Proceedings of the North American Manufacturing Research Institution of the Society of Manufacturing Engineers*. 2002, p. 8.

- [21] Lee K, Dornfeld DA. Micro-burr formation and minimization through process control. *Precis Eng* 2005; 29: 246–252.
- [22] Mian AJ, Driver N, Mativenga PT. Identification of factors that dominate size effect in micro-machining. *Int J Mach Tools Manuf* 2011; 51: 383–394.
- [23] Kiswanto G, Zariatin DL, Ko TJ. The effect of spindle speed, feed-rate and machining time to the surface roughness and burr formation of Aluminum Alloy 1100 in micro-milling operation. *J Manuf Process* 2015; 16: 435–450.
- [24] Lekkala R, Bajpai V, Singh RK, et al. Characterization and modeling of burr formation in micro-end milling. *Precis Eng* 2011; 35: 625–637.
- [25] Filiz S, Conley CM, Wasserman MB, et al. An experimental investigation of micro-machinability of copper 101 using tungsten carbide micro-endmills. *Int J Mach Tools Manuf* 2007; 47: 1088–1100.
- [26] Fang FZ, Liu YC. On minimum exit-burr in micro cutting. *J Micromechanics Microengineering* 2004; 14: 984–988.
- [27] Cutter N. Speeds and Feeds
<http://www.niagaracutter.com/solidcarbide/speedfeed.html>.
- [28] Ross PJ. *Taguchi Techniques for Quality Engineering*. New York: McGraw-Hill, 1998. Epub ahead of print 1998. DOI: 10.2307/1270793.
- [29] Prasad CS. *Finite element modeling to verify residual stress in orthogonal machining*. Blekinge Institute of Technology, Karlskrona, Sweden
<https://www.diva-portal.org/smash/get/diva2:830789/FULLTEXT01.pdf> (2009).